4.8 CHLOROPHYLL TRIPLETS AND RADICAL PAIRS

Alexander Angerhofer

TABLE OF CONTENTS

I. INTRODUCTION

Trying to review the immense amount of scientific research done on the subject of triplet and radical pair states in the field of photosynthesis during the last 20 years is quite a challenge, especially given the limited space available for the subject in this volume. Fortunately, some very good reviews of different parts of the field have been published which summarize most of the work done up to about 1986.[1-23] A number of references[1-5,7,10,11] review the magnetic resonance work done on the triplet state of chlorophylls *in vivo* and *in vitro* up to about 1982. The electron spin resonance (ESR) results on the components of the radical pair state in photosynthesis, especially the unique electron spin polarization (ESP), is reviewed up to about 1986.[3,6,7,17,18,23] References 8 and 9 deal with the electron nuclear double resonance (ENDOR) technique and its application to the research on photosynthesis (also see Chapter 4.7 in this book). For a review of the theoretical models of the primary charge separation as well as the involved molecules, updated to about 1987, see References 15 and 21. For other experimental work done on the electron transfer within reaction centers (RC) and model sytems as well as more general aspects of the primary steps in photosynthesis, please refer to References 12—14, 16, 19, 20, and 22 which are up to date through 1987, and to Chapters 4.10 and 5.3. This review concentrates on work done by application of magnetic resonance to the triplet state of chlorophylls, since the optical work is dealt with elsewhere (see Chapters 4.1 and 4.9). It does not aim to be exhaustive in giving details on every special area in this broad field, but, rather, presents an overview of what has been achieved in the last few years by the application of magnetic resonance on photosynthetic pigments, model systems, and pigment-protein complexes. For a more detailed in-depth review solely on the triplet state of chlorophylls, the reader is referred to an upcoming article in *Biochimica Biophysica Acta* by Thurnauer and Budil.[24]

A. THE TRIPLET STATE OF PHOTOSYNTHETIC PIGMENTS AND ITS ROLE IN PHOTOSYNTHESIS

The most important energy levels and relaxation pathways involved in the optical excitation of native and chemically reduced photosynthetic RCs of purple bacteria are shown in Figure 1. After excitation to the first excited singlet state, either by direct light absorption or energy transfer from an antenna (AT) pigment, the primary charge separation takes place, involving the intermediate electron acceptor H, a bacteriopheophytin (BPhe), and resulting in the reduction of the primary acceptor, a quinone species, about 200 ps after the initial excitation. If the RCs are isolated and there is no provision for either external electron donation to the primary donor P or a secondary acceptor to oxidize Q, the electron will eventually move back with a decay time of about 20 ms. Obviously, there is no triplet state involved in this scheme, and it has been clear now for many years that the triplet state does not participate in the primary step of photosynthesis. According to Figure 1A, the triplet state should not be observed in native RCs, which is true if one considers biochemical concentrations. Trace amounts of RC triplet have been observed, however, in native chromatophores of photosynthetic bacteria by the very sensitive method of fluorescence-detected magnetic resonance (FDMR).[25,26] This probably originates from a very low concentration of light-reduced RCs.

Although the triplet state does not occur naturally during the primary electron transfer process, it can be generated by adequate preparative methods. Since it is sensitive to various kinds of intermolecular interactions, it has been used widely as an intrinsic nondestructive probe of the intricate makeup of photosynthetic pigment-protein complexes. In order to form the triplet state in RCs in measurable concentrations, the complexes have to be reduced chemically or photochemically with sodium dithionite or ascorbate and light excitation. By this procedure, the quinone which serves as primary electron acceptor acquires an electron from the "outside world" and thus blocks the full charge separation of the primary process.

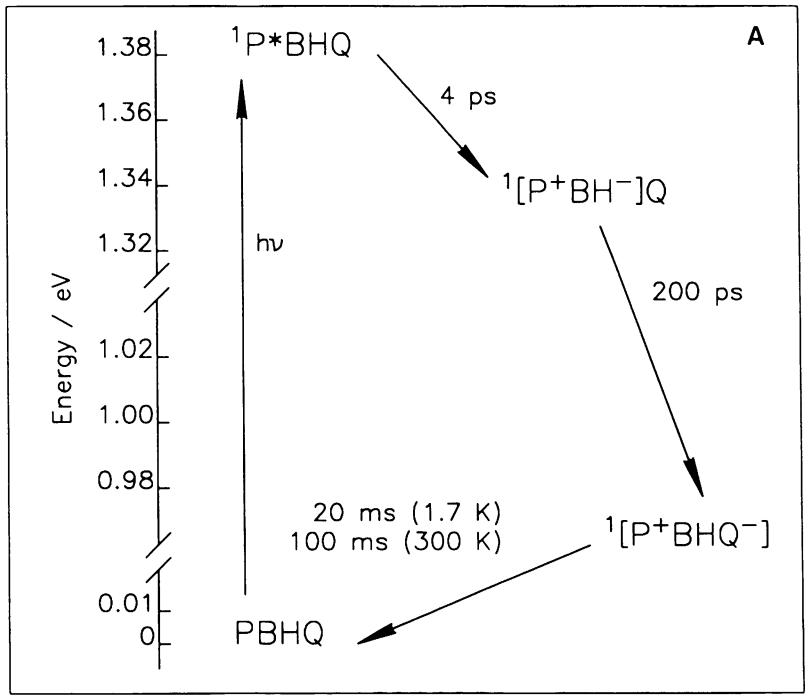

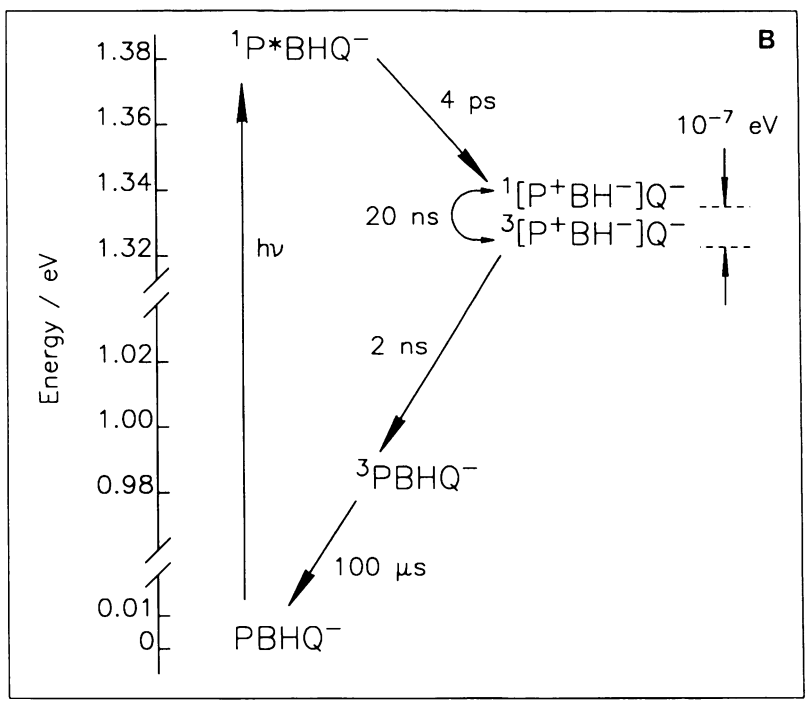

FIGURE 1. (A) Schematic representation of the excited states during the primary charge separation in native RCs.[3,205] (B) Schematic representation of the excited states during the primary charge separation in prereduced RCs.[27] P: BChl dimer, special pair, primary electron donor; B: BChl monomer, accessory monomer on the protein L-side; H: BPhe monomer, intermediate acceptor on the protein L-side; Q: ubiquinone-iron complex, primary electron acceptor.

As can be seen in Figure 1B, the electron which is ejected by the primary donor can only move as far as the intermediate acceptor H. From there, it has at least two major decay channels back to the ground state. It will recombine either by temperature-activated back-reaction into the excited donor singlet state with concurrent delayed fluorescence or by a spin-flip process into a triplet radical pair state P^+H^- with concurrent backreaction to the primary donor triplet state and, eventually, radiative or radiationless decay into the ground state. Backreactions involving the accessory bacteriochlorophyll (BChl) molecules as well as radiationless singlet-singlet recombination have been discussed also.[27] The backreaction to the triplet state of P is promoted by the radical pair mechanism, which can be readily seen from the ESP pattern, given the knowledge of the sign of D.[2,6,28] The formation of the triplet state comes about in the charge-separated state by singlet-triplet mixing through hyperfine interactions and g-value differences. The triplet state generation in photosynthetic pigments in antenna (AT) complexes as well as *in vitro*, however, is governed by spin-orbit mixing of singlet and triplet states.

Once the triplet state is generated *in vivo*, it can be analyzed and its characteristics have to be compared to *in vitro* data of the respective pigments. Careful study of the triplet state of these molecules in different environments (organic solvents, aggregates, protein matrices, etc.) yields a data set against which the *in vivo* data must be compared to obtain information about the molecular and electronic structure of the pigments involved in the primary step of photosynthesis. The zero-field splitting (zfs) or fine structure as well as the intersystem crossing (ISC) rates are strongly influenced by intermolecular interactions. The ESP gives information about the radical pair state out of which the triplet is born. The triplet state has also been used as a detection probe for magnetic resonance of the radical pair by reaction yield-detected magnetic resonance (RYDMR). Extensive use of the triplet state as a built-in sensor has been made to yield spectroscopic information on the whole complex with methods like microwave-induced absorption (MIA), linear dichroism absorption-detected magnetic resonance (LD-ADMR), or microwave-induced fluorescence (MIF). In ENDOR experiments, the triplet state has been used to map out the delocalization of the electrons over the special pair molecules. Single-crystal EPR studies have revealed the geometry of the fine-structure tensor relative to the molecular axes of the primary donor.

B. THE ROLE OF RADICAL PAIR STATES IN PHOTOSYNTHESIS

As is obvious from Figure 1A, the primary step of photosynthesis involves at least two different radical pair states, a hole on the primary donor and an electron on either the intermediate acceptor H or the primary acceptor Q. Naturally, the interaction between both unpaired electrons grows weaker the farther they are apart. One has to distinguish between the singlet and triplet radical pair, which are separated in energy by 2 J, with J on the order of 6 to 10 Gauss (18 to 30 MHz) at the distances involved. Both forms undergo rapid interconversions through hyperfine and Δg-mixing of singlet and triplet levels. Recombination occurs mainly through the triplet channel, whose lifetime has been calculated from RYDMR data to about 2 ns, compared to about 20 ns for the singlet lifetime. This leads to a characteristic ESP which can be detected by magnetic resonance. Since the level splitting and the relaxation rates of these states are highly sensitive to intermolecular interactions, much research has been focused on this state to figure out D, E, and J, the main parameters of electronic interaction.

Numerous publications deal with the investigation of model radical pairs to gain insight into the mechanisms and kinetics of the electron transfer dominating many chemical reactions. Since the RC has been studied so well and detailed geometric structure from X-ray crystallography is available, it can be used as a model system for redox reactions as well.

II. THEORY

A. THE TRIPLET STATE

1. Fine Structure

The electronic states of the chlorophylls in the visible and near-UV spectral range are qualitatively well described by Gouterman's four-orbital model (for reference, see Chapter 4.9). After the usual separation between space and spin coordinates, the triplet state can be described by the three-spin functions $|T_{+1}>$, $|T_0>$, $|T_{-1}>$ or $|\tau_x>$, $|\tau_y>$, $|\tau_z>$, depending on the applicability of the high-field or low-field approximation. The energy separation between the first excited singlet and triplet states is determined by the exchange integral J, with ψ_0 and ψ_1 denoting the wavefunctions of the highest occupied molecular orbital (HOMO) and lowest unoccupied molecular orbital (LUMO) and the electrons indicated in parentheses.

$$J = \left\langle \psi_0(1) \cdot \psi_1(1) \left| \frac{e^2}{r_{12}} \right| \psi_0(2) \cdot \psi_1(2) \right\rangle \tag{1}$$

The degeneracy of the three triplet sublevels is lifted by spin-spin interactions (fine structure, hyperfine structure, and spin-orbit interaction) and external magnetic fields if applied. For simplification, only the dipolar coupling and the Zeeman-splitting is considered, since these terms provide the largest contribution to the sublevel splitting anyway. In this case, the Hamiltonian is written as

$$\hat{H} = g \cdot \mu_B \cdot \{\hat{S}_1 + \hat{S}_2\} \cdot B + \hat{S}_1 \cdot \hat{\mathbf{D}} \cdot \hat{S}_2 \tag{2}$$

where **D** is the fine-structure tensor. By diagonalization of the Hamiltonian along the fine structure tensor axes, the dipolar part can be represented in a very simple form:

$$\hat{H}(B = 0) = \hat{S}_1 \cdot \begin{pmatrix} (D - E) & 0 & 0 \\ 0 & (D + E) & 0 \\ 0 & 0 & 0 \end{pmatrix} \cdot \hat{S}_2 \tag{3}$$

With an external magnetic field B_0 pointing in an arbitrary direction from the molecular axes, the matrix elements of the Hamiltonian are

$$H_{uv} = \begin{pmatrix} (D - E) & -irg\mu_B B_0 & iqg\mu_B B_0 \\ irg\mu_B B_0 & (D + E) & -ipg\mu_B B_0 \\ -iqg\mu_B B_0 & ipg\mu_B B_0 & 0 \end{pmatrix} \tag{4}$$

with p, q, and r the direction cosines of the magnetic field with reference to the molecular frame ($p = \cos\{B_0,x\}$; $q = \cos\{B_0,y\}$; $r = \cos\{B_0,z\}$). D and E are the zero-field splitting (zfs) or fine structure parameters. By performing the integration over the space coordinates, they can be expressed as:

$$D = {}^3/_4 \cdot g^2 \cdot \mu_B^2 \cdot \left\langle \frac{r_{12}^2 - 3z_{12}^2}{r_{12}^5} \right\rangle \tag{5a}$$

$$E = {}^3/_4 \cdot g^2 \cdot \mu_B^2 \cdot \left\langle \frac{y_{12}^2 - x_{12}^2}{r_{12}^5} \right\rangle \tag{5b}$$

$r_{12} = \sqrt{(x_{12} + y_{12} + z_{12})^2}$ is the distance between both electrons. As can be seen from these equations, D and E provide a measure of the distribution of both spins across the molecule. The most popular convention for choosing the molecular axes in aromatic molecules is to have the z-direction pointing perpendicular to the π-plane. Since in most cases $z_{12} < x_{12}, y_{12}$, D provides a measure of the average distance between both electron spins, whereas E is a measure of the asymmetry of the wavefunction in the x,y-plane.

2. Intersystem Crossing

In pure spin states (i.e., time-independent spin states), such as the ones discussed above, there is no provision for transitions between singlet and triplet states due to angular momentum conservation. These transitions are "spin forbidden", which leaves them weaker in intensity by several orders of magnitude in experimental observation than transitions within a multiplet. ISC between singlet and triplet systems is, however, facilitated by spin-orbit coupling (SOC), or the radical pair mechanism (RPM) which is the dominant ISC process in photosynthetic RCs. SO interaction is essentially a relativistic quantum mechanical effect which results from the interaction between the electron orbit-induced magnetic field and the magnetic field of the spin. Obviously, only the field along the spin axis contributes to the effect. The nonvanishing dot product between spin and orbit momentum is brought about by the asymmetry in the charge distribution of the relativistic electron. The law of angular momentum conservation then applies to the sum of spin and orbital momentum, which allows for time-dependent "reshuffling" of angular momentum between spin and orbit. In the case of weak SOC, which is true for most aromatic molecules (the orbital momentum is quenched), it can be viewed as a small perturbation slightly mixing singlet and triplet states with each other.

In the case of large planar aromatic molecules like Chl, some statements can be made about SOC and its effect on ISC:

1. The heavy atom effect: the larger the nuclear charge, the larger is the magnetic field felt by the electron on its orbit and, hence, the larger is the SOC.
2. The more orbital overlap the electron has with the nucleus, the larger the SOC will be. Therefore, s-orbital electrons will experience larger SO interactions than p-orbital electrons.
3. Quenching of orbital momentum: due to the large extension of the π-orbitals in planar aromatic molecules and their comparably small overlap with the nuclei, the resulting orbital momentum is very small (compared to an atom or a small molecule). This reduces SOC considerably.
4. Obviously, SOC is dependent on the direction of the resulting electron spin of the two unpaired electrons. It varies dramatically between the three triplet sublevels. In planar aromatic molecules without heavy atom effects, the z-level usually has the weakest SOC, since the one-center SO integrals tend to cancel each other out because of the D_2 symmetry with the molecular plane as the plane of symmetry.

B. CHARGE-TRANSFER AND RADICAL PAIR STATES

Following the theoretical description of Budil,[29] the parts of the total Hamiltonian which govern the dynamics of the involved electron spins are the Zeeman term, spin-spin interaction consisting of a dipolar and an exchange term, and anisotropic hyperfine interaction with surrounding nuclei.

$$\hat{H} = \sum_i \hat{S}_i \cdot \mathbf{g}_i \cdot B_0 + \sum_{j>i} \{-J_{ij} \cdot (^1/_2 + 2\hat{S}_i \cdot \hat{S}_j) + \hat{S}_i \cdot \mathbf{D}_{ij} \cdot \hat{S}_j\} + \sum_{i,m} \hat{S}_i \cdot \mathbf{A}_{im} \cdot \hat{I}_m \quad (6)$$

The terms used in this equation are B_0 = externally applied magnetic field; $\hat{S}_{i,j}$ = electron spin operators; $\hat{I}_m$ = nuclear spin operators; $\mathbf{g}_i$ = anisotropic electron g-tensor; J_{ij}

= electronic exchange interaction; $\mathbf{D}_{ij}$ = anisotropic electron fine-structure tensor; $\mathbf{A}_{im}$ = anisotropic hyperfine interaction tensor. The summation is done over each one of the involved paramagnetic electrons with spin S_i,S_j and over each involved paramagnetic nucleus I_m. Except for hyperfine interaction, all other nuclear parts of the Hamiltonian are neglected due to their smallness compared with the electronic part. Electronic spin-orbit coupling is represented within an effective anisotropic g-tensor in the electronic Zeeman part. For further simplification, the paramagnetic iron is neglected, which leaves the total number of unsaturated electron spins at two or three, depending on the reduction state of the quinone acceptor.

By following Schulten and Wolynes' approach,[30] the hyperfine interaction can be treated as a constant magnetic field vector, assuming that no nuclear spin-flips take place during the lifetime of the radical pair. The small anisotropy (<1 G) of the hyperfine couplings is also neglected in this simplified treatment, allowing for purely isotropic A_{im}. Now the electronic states have to be averaged over an appropriate distribution of the hyperfine vectors.

The time-dependent Schrödinger equation with the above Hamiltonian can be evaluated, e.g., with the density matrix representation,[29] and the actual physical observables have to be calculated, using the crystal structure data, and compared to the experiment. The parameters g, J, D, k_T, and k_S are obtained by best fits to all available experimental results. This data set then serves as the best explanation to all experimental observations and is regarded as the true data set. Some of these parameters can be calculated from the structure coordinates of the pigments and coincide well with the parameters obtained from the fit.

III. THE TRIPLET STATE OF PHOTOSYNTHETIC PIGMENTS *IN VITRO*

A. MONOMERS

In order to understand the complex interactions of the Chl pigments in a photosynthetic pigment-protein complex, the influence of the surrounding environment on the triplet state of the single molecule has to be understood. Since the wavefunction of the conjugated π-electron ring is confined to the porphyrin skeleton, interactions with the phytyl chain should influence the triplet state only indirectly (e.g., by insertion of the phytyl chain in a detergent micelle, complexation of Chl molecules is likely to take place). Attention is therefore focused on the direct interactions, which are divided into ligand effects, metal ion substitution, hydrogen bonds at the keto and carbonyl groups of the ring, and insertion into liquid crystals.

1. Ligand Effects

The central Mg atom of Chls is found in either the penta- or hexacoordinated form. The in-plane ligation is provided by the four nitrogen atoms of the pyrrole rings, whereas the out-of-plane ligation comes from either one or two solvent molecules (or other Chls, water, etc.). There are distinct changes in the optical spectrum accompanying the change from the penta- to the hexacoordinated state, which have qualitatively been accounted for by Rebeiz and Bélanger.[31,32] BChl, especially, has long been known for a large bandshift of its Q_x absorption band upon change in coordination number.[33-35] These optical differences as well as evidence from resonance Raman measurements[35,36] can be used to determine the coordination state of the Chl. The magnetic resonance data shown in Table 1 on the different coordination states are thus based on the optical identification.

The identification of the coordination state of Chl **b** does not seem to be very clear (see Table 1). However, the results on Chl **a** and BChl **a** show a reduction in |D| and |E| of at least 3 and 10%, respectively, with increasing coordination number of the Mg atom from 5 to 6. These differences are well resolved with high-resolution, zero-field optical-detected magnetic resonance (ODMR) spectroscopy. Comparison with the triplet parameters of photosynthetic pigment-protein complexes *in vivo* shows that the chlorophylls in these complexes are mostly present in their pentacoordinated state,[37,39] a result that is substantiated by res-

TABLE 1
Triplet State Parameters of Chlorophylls in Organic Solvents Which Put the Central Mg Atom in Different Coordination States C

Molecule	Solvent	Temp (K)	|D| (10^{-4} cm^{-1})	|E| (10^{-4} cm^{-1})	k_x, k_y, k_z, k_T (s^{-1})	C	Ref.
Chl **a**	*n*-oct./H_2O	2	299.2 ± 2	44.4 ± 2	295 ± 20, 585 ± 40, 35 ± 5, 330 ± 20	5	37
			277.2 ± 2	34.7 ± 2	660 ± 50, 1250 ± 100, 150 ± 10, 710 ± 50	6	
	Pyr		275 ± 2	36.5 ± 2	780 ± 40		
			281.5 ± 2	39.0 ± 2			
	Dry Pyr				630		41
	Wet Pyr				1111	5	
Chl **b**	*n*-oct./H_2O		325.2	35.0	380 ± 40	6	38
			341.1	34.2	360 ± 40	?	
			326.4	36.2	160 ± 10	5	
BChl **a**	Tol/Pyr	1.2	229 ± 1	57 ± 1		6	39
	DEE		239 ± 1	73 ± 1		5	
			231 ± 1	59 ± 1		6	

Note: *n*-oct. = *n*-octane; Pyr = pyridine; Tol/Pyr = 90% toluol/10% pyridine; DEE = diethylether; k_i (i = x, y, z) are the sublevel decay rates and k_T, the overall observed triplet decay rate. k_T is given when only 1 number appears in column 6.

TABLE 2A
Triplet State Lifetimes τ_T of Chl a Measured at 77 K by the Fluorescence-Fading Method When Recording Is Set at λ_m

Solvent	λ_{exc} (nm)	λ_{flu} (nm)	Δ (nm)	λ_m (nm)	τ_T (ms)	Type of solvate[a]
γ-Collidine	457.9	679.6[b]	18.8[b]	685	1.2	L_2
	514.5	674[b]	17.6[b]	665	3.0	L_1
t-Butanol	457.9	675	17.4	—	—	L_1H
	514.5	675	16.7	677	2.2	L_1H
TEA/H_2O	457.9	682	12.1	682	0.95	L_2H
	514.5	672	16.4	672	2.5	L_1H

Note: λ_{flu} and Δ are the fluorescence band-peak maximum and its FWHM when excitation is fixed at λ_{exc}. TEA = triethylamine; TEA/H_2O = TEA + ≤0.5% H_2O.

[a] Solvate types preferentially excited at λ_{exc} or detected at λ_m. L_i denotes the coordination number (= i + 4) of the central Mg atom. L_1H denotes additional hydrogen bonds.

[b] At 5 K.

onance Raman data as well. A qualitative explanation of the decrease in D and E on increase of the coordination number was given by Clarke et al.[40] The attachment of an additional ligand to the central Mg atom allows for a greater delocalization of the π-electrons over the conjugated ring because of reduced attraction to the center. Greater delocalization, of course, results in lower zfs values.

The dependence of the ISC rate on ligation has been evaluated semiquantitatively by Bowman.[41] According to his analysis, ISC in chlorophylls and pheophytins is determined by out-of-plane distortions at the four nitrogen atoms, i.e., by N-H vibrations (in the case of pheophytin) or by the size and specific solvent interaction of the central metal atom. With the Mg located more in the macrocycle, as is the case in the hexacoordinated form, the molecule would exhibit smaller ISC rates, which can be verified from his experiments (see Table 1). This does not agree with other published results. In fact, Mauring et al.[50] pointed out that the dependence of the triplet decay time on the ligation state can simply be interpreted with the energy gap law which predicts shorter ISC times with a smaller energy gap between T_1 and S_0. This is substantiated by a wealth of triplet decay measurements on Chl **a** and pyrochlorophyll (pyro-Chl) **a** in a huge number of different solvents.[50] Mauring et al. explain the differing results with a wrong assignment of the pentacoordinate form to the fast-decaying triplet state by Bowman. However, Mauring's assignments of the pigment coordination state are also based on their absorption spectra. This can be hazardous in the case of plant chlorophylls, since the observed differences are small and not very well founded by additional independent information (e.g., resonance Raman data). Nevertheless, Mauring et al. were able to show clearly that the ISC rates of different chlorophyll species follow the energy gap law well, even within the inhomogeneous fluorescence band of one spectral form, whatever its assignment might be. They derive the following relationship between triplet decay time τ_T and the energy gap $\Delta E(T_1 - S_0)$:

$$\text{Log}\tau_T[s] = -7.88 + 5 \times 10^{-4} \cdot \Delta E(T_1 - S_0)[cm^{-1}] \quad (7)$$

Some representative data of Mauring's are listed in Tables 2A to 2C.

2. Effects of the Central Metal Atom

In photosynthesis, one deals with chlorins or bacteriochlorins that contain a Mg atom

TABLE 2B
Triplet State Lifetimes τ_T of PCl as Measured at 77 K by the Fluorescence-Fading Method When Recording Is Set at λ_m

Solvent	λ_{exc} (nm)	λ_{flu} (nm)	Δ (nm)	λ_m (nm)	τ_T (ms)	Type of solvate[a]
Pyridine	457.9	642	14.3	640	4.5	L_2
	514.5	630, 642	21	625	9.2	L_1
				635	7.7	L_1
				645	6.0	L_2
Methanol	457.9	643	19.1	635	3.72	L_2H
				645	2.62	L_2H
				655	2.2	L_2H
	514.5	633.5	20.1	620	9.6	L_1H
				625	8.32	L_1H

Note: λ_{flu} and Δ are the fluorescence band-peak maximum and its FWHM when excitation is fixed at λ_{exc}.

[a] Solvate type for which τ_T was measured. Notation as in Table 2A.

TABLE 2C
Triplet State Lifetimes τ_T (ms) of Chl a Measured at 77 K by the Fluorescence-Fading Method When Recording Is Set at λ_m (left-most column) and the Excitation Wavelength at λ_{exc} (second row)

λ_m (nm)	TEA (514.5 nm)	Pyridine (457.9 nm)	CH_3OH (457.9 nm)	CD_3OD (457.9 nm)
655	4.38			
660	3.13			
665	2.88	1.72	1.2	
670	2.50	1.71 (1.61)	1.37 (1.43)	
675	2.46	1.52 (1.52)	0.94 (1.08)	1.05
680	2.58	1.35 (1.38)	0.77 (0.95)	1.04
685		1.25 (1.17)	0.77 (0.90)	0.93
690		1.15		

Note: The corresponding τ_T values for fully deuterated solvents are indicated in parentheses. TEA = triethylamine.

as the central metal or are present in the free base (pheophytins). For an understanding of the optical and magnetic properties, it proved helpful to synthesize molecules with different central metal atoms, Zn being a prominent example. Table 3 lists the triplet state properties of chlorophylls with either none (pheophytins) or various different metal atoms.

For the Chl **a** system, there seems to be a consistent increase in |D| and |E| on replacement of Mg by Zn. This is not the case for Chl **b**. Except for Ca-Chl **b**, the |D| values stay within 3% of the Mg-Chl parameter. The huge difference for Ca-Chl **b** can be explained by the size of the Ca atom. Since it is the largest of the employed ions, it is located considerably out of the plane of the molecule, which also makes it much more prone to demetalation. This out-of-plane location could provide increased interactions with the π-electrons on the ring, thus reducing their delocalization and increasing D.

The behavior of the ISC rates can be qualitatively understood within the frame of radiationless triplet state relaxation of large planar aromatic molecules.[41,47-49] In the ideal

TABLE 3
Triplet Parameters of Chlorin Rings Substituted with Different Central Metal Atoms

Ring	Atom	T (K)	|D| (10^{-4} cm^{-1})	|E| (10^{-4} cm^{-1})	k_x, k_y, k_z (s^{-1})	p_x:p_y:p_z	Ref.
Chl **a**	H_2	100	341 ± 5[a]	33 ± 3	1,040 ± 50, 1,300 ± 100, 820 ± 100	0.72:1:0.6	42
	Mg	2	280 ± 3[b]	38 ± 3	661 ± 89, 1,255 ± 91, 241 ± 15	0.3:1:0.1	43
	Zn		306 ± 3[b]	42 ± 3	346 ± 50, 330 ± 32, 660 ± 70		
pyro-Chl **a**	Mg	100	281[c]	28		0.8:1:0.25	44
	Zn	116	309[c]	38		1.0:0:1.0	
Chl **b**	H_2	100	358 ± 8[a]	46 ± 5	590 ± 50, 870 ± 150, 420 ± 150	0.63:1:0.48	42
	H_2	2	368 ± 8[b]	49 ± 4	311 ± 44, 1,000 ± 24, 54 ± 5		46
	Mg		320 ± 10[b]	41 ± 6	268 ± 34, 570 ± 54, 34 ± 4	0.3:1:0	43
	Zn		328 ± 3[b]	32 ± 3	122 ± 13, 250 ± 50, 622 ± 47	0.3:0.7:1	45
	Ca		396 ± 8[b]	39 ± 6	207 ± 24, 480 ± 38, 32 ± 6		46
	Cd		326 ± 5[a]	36 ± 3	370 ± 27, 462 ± 37, 722 ± 50		

Note: k_i (i = x, y, z) are the triplet sublevel decay rates; p_i (i = x, y, z) are the respective population probabilities.

[a] In methyltetrahydrofurane.
[b] In *n*-octane.
[c] In liquid crystal type E-7.

case of a planar molecule, the one-center spin-orbit integrals cancel each other out. This is, however, not entirely the case if the planarity is disturbed. A slight puckering of the molecule will allow the in-plane spin sublevels to be depopulated more rapidly by nonvanishing one-center SOC. Therefore, k_x and k_y are expected to be larger than k_z, which is the case for most planar aromatic molecules. The rates of the Phe **a/b**, Chl **a/b**, PChl **a**, and Ca-Chl **b** follow this prediction well. In the case of Zn- and Cd-substituted chlorophylls, however, the out-of-plane sublevel (z) is the dominant depopulation channel. This behavior can be understood by the interaction of the metal d-electrons with the nitrogen electrons which are mostly responsible for SOC. In this manner, the out-of-plane spin-orbit component acquires nonvanishing one-center integrals, which result in a dramatic increase of the k_z rate. In fact, k_z almost doubles k_x and k_y in this case.

3. Effects of Hydrogen Bonds

To date, not very much attention has been paid to the effect of hydrogen bonds at the periphery of the macrocycle on the triplet state parameters. Hydrogen-bonding of solvent molecules at the carbonyl oxygen of the isocyclic ring changes the optical absorption of Chl **a** markedly.[51] The effect on the ISC rates, however, is negligible, as was shown by Mauring et al.[50] in a kinetic study using partially deuterated solvents. However, in the case of the hexacoordinated form, additional hydrogen bonds from the ligating solvent molecule's O-H group to the pyrrole-nitrogen atoms is proposed to be the reason for a quite drastic increase in the ISC rate in L_2H complexes (see Table 2A, B). Mauring et al. argue that higher overtones of the O-H stretching vibrations in these solvent molecules at least partially acquire triplet character, thus facilitating ISC.

4. Chlorophyll in Liquid Crystals

If crystallization of organic molecules is impossible or very difficult to perform, as is the case with some chlorophylls due to their aliphatic phytyl chain, another method to obtain at least partially ordered molecular arrangements are liquid crystals. They have been used frequently to incorporate guest molecules to determine molecular ordering and orientational parameters as well as anisotropic optical and magnetic properties.[52,53] Using time-resolved ESR techniques, the ESP of chlorophylls incorporated in liquid crystalline matrices as well as the characteristic relaxation times T_1 and T_2 have been measured (see Table 4).

Note the difference in population probabilities on substitution of the central Mg atom with Zn, which leads to a different ESP pattern. The reason for this behavior was discussed in the preceding paragraph.

B. AGGREGATES

Aggregates of chlorophylls have long been known to partly resemble the spectroscopic properties of native pigment-protein complexes. For this reason, they have been used as model complexes to mimic and investigate the geometrical and spectroscopic makeup of photosynthetic pigments in RCs and ATs. The triplet-state data of these aggregates have been used to evaluate their structure, but also as a reference for triplet data of *in vivo* complexes.

1. Chlorophyll Dimers

The chlorophyll molecule is uniquely suited to form aggregates through ligand and hydrogen bonds by its central Mg atom and carbonyl ring substituents. Since the electron donor of the bacterial RC had been proposed to be a BChl dimer,[58,59] the so-called "special pair", models for such a dimer were suggested using water as the bridge linking both molecular planes together by hydrogen and ligand bonds.[60-62] Aggregates without water, using the ring carbonyl oxygens as ligands for the central Mg atom of the neighboring molecule, have also been discussed.[63] Another method of linking two chlorophylls together

TABLE 4
Triplet State Parameters of Chlorophylls in Liquid Crystalline Matrices

Molecule	T (K)	$\|D\|$ (10^{-4} cm^{-1})	$\|E\|$ (10^{-4} cm^{-1})	k_x, k_y, k_z (s^{-1})	k_T (s^{-1})	$p_x:p_y:p_z$	T_1 (μs)	T_2 (μs)	Ref.
Chl **a**[a]	100	286	38	1200, 840, 360	800	1:0.9:0.4	200	0.9	54
pyro-Chl **a**[a]		281	28			0.8:1:0.25			44
Zn-pyro-Chl **a**[a]	116	309	38			~1:~0:~1			
Zn-pyro-Chl **b**[a]	100	328	32			0.3:0.7:1			55
Chl **a**[b]	300	284	40			0.36:0.44:0.2	0.075	0.01	56, 57
	130						20.2	1.0	

Note: k_i (i = x, y, z) are the triplet sublevel decay rates; k_T is the overall observed triplet decay rate; p_i (i = x, y, z) are the triplet sublevel population probabilities; T_i (i = 1, 2) are the characteristic longitudinal and transversal decay times. For the source of the liquid crystals, refer to the respective references.

[a] In liquid crystal type E-7.
[b] In liquid crystal type 85-1084.

is just by covalent bonds.[64] Upon optical excitation, these dimeric or oligomeric species readily form triplet states which can be observed optically[65-67] as well as with magnetic resonance methods.[68-72] Attempts to elucidate the geometrical structure of the special pair from its fine structure and triplet dynamics[68,72] on the basis of the method of Sternlicht and McConnell[73] later proved to be erroneous, since charge transfer (CT) contributions have to be taken into account.[5,74] Since the magnitude of these CT contributions to the electronic wavefunction cannot be determined by electron paramagnetic resonance alone in a simple way, the fine structure data of the RC cannot serve as a reliable source for geometrical information. Triplet state data of synthetic dimers are found in Table 5.

A description of the triplet state parameters of synthetic dimers of Chl **a** and Phe **a** incorporating CT effects was given by Kooyman and Schaafsma,[74] who developed the charge-resonance exciton model for dimers. Structural information gained from that approach coincided well with results from NMR.[5]

2. Chlorophyll in Micelles

Detergent micelles and lipid vesicles have become increasingly popular as a matrix to study aggregation and electron transfer (ET) properties of photosynthetic molecules. Their optical spectroscopic properties (absorption, fluorescence, CD, etc.) especially resemble those of pigments *in vivo* and are therefore studied as model systems.[76-79] It is also well established that Chl triplet states serve as electron donors in the presence of suitable acceptors within such an environment. This reaction is diffusion controlled[80,81] at high temperatures, but also occurs in frozen (see also Chapter 1.12). Triplet state parameters of chlorophylls in a micellar environment are listed in Table 6.

The results of Hotchandani et al.[83] were interpreted with mono- and biligated forms of Chl **a** (see Section III.A.1) occurring in the vesicles, whereas those of Hiromitsu et al.[84] reflect the effect of higher Chl **a** concentration on the triplet parameters. The first line of data of Hiromitsu et al.[84] in Table 6 was interpreted as originating from monomeric Chl **a**, whereas the decrease in D and the increase in decay rates in the second line was interpreted with spectral diffusion of the triplet state between two or more Chl **a** molecules. The ESP pattern of the Chl **a** triplet state in frozen egg-phosphatidylcholine vesicles resembles that in polycrystalline matrices. Differences are seen, however, in the x-component of the powder spectra. This seems to reflect the partially ordered local environment of the chlorin ring near the lipid bilayer surface.

3. Chlorophyll in Proteins

Chlorophyll-protein interactions seem to play a fundamental role in the primary electron transfer process of photosynthesis. The protein provides the geometrical structure which is the basis for photosynthetic action. The influence of the protein environment on the Chl spectroscopic properties has been studied in great detail by resonance Raman spectroscopy (see Chapter 4.6). Magnetic resonance studies of pigments in a protein environment other than the native photosynthetic complexes was done mostly by FDMR in zero field. Data are listed in Table 7.

The main result of Clarke's work with pyrochlorophyllide (pyro-Chlid) **a** in apomyoglobin was the assignment of the different spectral forms to five- and six-coordinated pigments[85] (also see Section III.A.1). Both conformations seem to be interconvertible at room temperature, as suggested by NMR data,[88] but freeze at very low temperatures. The work of Beck et al.[86] was done on biosynthetic precursor complexes containing molecules of the different biosynthesis steps of BChl.[89] These pigments are bound in membrane proteins, presumably precursor proteins of the photosynthetic protein complexes. From the ODMR data, it was concluded that at least BChl **a** (or BChlid **a**) is present in its pentacoordinated form within this protein. The work of Hala et al.[87] was concerned mainly with the interactions between pheophytin covalently bound to synthetic polyamino acid. Comparison of the triplet

TABLE 5
Triplet Parameters of Dimers and Oligomers of Chlorophylls and Pheophytins

Molecule	T (K)	λ_{det} (nm)	|D| (10^{-4} cm^{-1})	|E| (10^{-4} cm^{-1})	k_x, k_y, k_z (s^{-1})	k_T	Ref.
Chl **a**	2	720	272[a]	36	732 ± 110, 980 ± 170, 180 ± 30	690 ± 50	67
		730	252[b]	39			
		760	266[c]	33			
Zn-Chl **a**		720	280[a]	39	525 ± 25, 585 ± 25, 1220 ± 50	800 ± 50	
(pyro-Chl **a**)$_2$		682	277[d]	36			
		733	268[d]	35	830 ± 100, 70 ± 80, 170 ± 20	690	
(Zn-pyro-Chl **a**)$_2$		675	300[d]	38	340 ± 20, 380 ± 20, 660 ± 40	470 ± 50	
		720	281[d]	34	600 ± 30, 620 ± 30, 1490 ± 60	980 ± 50	
(Chl **a** · H_2O)$_2$		725	286 ± 5[e]	31 ± 5			70
(Chl **a** · H_2O)$_n$		750	275 ± 5[e]	38 ± 6			
(Chl **b**)$_2$		700	281 ± 3[a]	31 ± 3			71
(Phe **a**)$_2$	4.2	713	324 ± 3[e]	16 ± 4			
(Phe **b**)$_2$	2	704	323 ± 5[e]	15 ± 5			
(Phe **a** · H_2O)$_2$	5—50		273 ± 5[f]	35 ± 6			75
Phe **a**			282 ± 5[g]	32 ± 2			
(Phe **b**)$_3$			277 ± 5[f]	32 ± 5			
(Chl **b** · MTHF)$_2$	4.2		255 ± 3[h]	69 ± 3			69
(Chl **b**)$_2$			272 ± 3[h]	41 ± 3			

Note: λ_{det} = fluorescence wavelength on which the FDMR signal was recorded; k_i (i = x, y, z) = triplet sublevel decay rates; k_T = overall observed triplet decay rate.

[a] In methylcyclohexane:pentane (1:1) with 10^{-2} *M* H_2O.
[b] In ethanol.
[c] In toluol + 10^{-2} *M* ethanol.
[d] In toluol:methanol (3:1).
[e] In *n*-octane.
[f] In methylcyclohexane.
[g] In toluol.
[h] In methyltetrahydrofurane.

TABLE 6
Triplet State Parameters of Chl a in Phosphatidylcholine (PC)

T (K)	λ_{exc} (nm)	λ_{det} (nm)	|D| (10^{-4} cm^{-1})	|E| (10^{-4} cm^{-1})	k_x, k_y, k_z (s^{-1})	k_T	p_x:p_y:p_z	Ref.
2	457.9	690	283	34		600 ± 50		83
	514.5	670	294	38		400 ± 40		
77	brdbd		283 ± 1[a]	35 ± 2	714 ± 4, 752 ± 5, 546 ± 107		0.949:1:0.714	84
			276 ± 2[b]	34 ± 2	1067 ± 1, 1128 ± 13, 966 ± 34		0.949:1:0.854	

Note: λ_{exc} = excitation wavelength in the FDMR experiment; λ_{det} = fluorescence wavelength on which the FDMR was detected; k_i (i = x, y, z) = triplet sublevel decay rates; k_T = overall observed triplet decay rate; p_i (i = x, y, z) = triplet sublevel population probabilities; brdbd = broadband excitation.

[a] Chl a:PC = 0.2:40.
[b] Chl a:PC = 1:40.

TABLE 7
Triplet State Parameters of Chlorophylls and Pheophytins in Different Amino Acid Matrices

Molecule	T (K)	λ_{exc} (nm)	λ_{det}	|D| (10^{-4} cm^{-1})	|E| (10^{-4} cm^{-1})	k_x, k_y, k_z (s^{-1})	k_T	Ref.
pyro-Chlid **a**	2	457.9	671	297[a]	37	814 ± 70, 714 ± 10, 31 ± 5	520	85
			685	284[a]	33	804 ± 70, 832 ± 25, 69 ± 8	568	
		514.5	668	300[a]	38			
BChl **a**	1.7	590	783	232[b]	69			86
BPhe **a**		530	760	265[b]	46			
2-desacetyl-2α-hydroxyethyl-BPheid **a**		514.5	718	280[b]	66			
Pheid **a**		514.5	674	334[b]	22			
Chlid **a**		610	667	299[b]	37			
2-desvinyl-2α-hydroxyethyl-Pheid **a**		501.7	661	340[b]	23			
2-desvinyl-2α-hydroxyethyl-Chlid **a**		624	659	308[b]	38			
Pheid **a**	4.2	brdbd	680	359 ± 2[c]	25 ± 1	1199 ± 47, 444 ± 24, 82 ± 6		87
				337 ± 2[d]	24 ± 1	1367 ± 135, 409 ± 31, 55 ± 9		
				359 ± 2[e]	27 ± 1			

Note: λ_{exc} = wavelength of excitation in the FDMR experiment; λ_{det} = fluorescence wavelength on which the magnetic resonance was detected; k_i (i = x, y, z) = triplet sublevel decay rates; k_T = overall observed triplet decay rate; brdbd = broadband excitation.

[a] In apomyoglobin.
[b] In a biosynthesis precursor protein.
[c] In a synthetic polyamino-acid (L-Lys-L-Ala-L-Ala)$_n$ in dimethylformamide.
[d] In dimethylformamide.
[e] In *n*-octane with 0.5% (vol/vol) ethanol.

TABLE 8
Triplet State Parameters of Chl b in LB Films

Sample	Substrate	MF	|D| (10^{-4} cm^{-1})	|E| (10^{-4} cm^{-1})	k_x, k_y, k_z (s^{-1})	k_T (77 K) (s^{-1})
a	HOPG	4×10^{-2}	320	34		
b		1×10^{-4}	321	35	601 ± 5, 582 ± 18, 48 ± 6	398 ± 20
c			323	32		
b	Glass		322	32		272 ± 18
Chl **b**	*n*-Octane		320	41	268 ± 34, 570 ± 54, 34 ± 4	292 ± 17

Note: MF = mole fraction of Chl **b**; k_i (i = x, y, z) = triplet sublevel decay rates; k_T = overall observed triplet decay rate at 77 K. For sample and substrate nomenclature, see text.

state data with data from organic solutions shows that the pigments are located in the nonpolar pockets of the folded amino acid chain (see Table 7). D and E correspond much more to the data found in the nonpolar organic solvent *n*-octane than to the data in the polar solvent dimethylformamide (DMF). Taking into account results from optical spectroscopy, Hala et al. succeeded in constructing a model of their complexes in which some of the pigments are buried in the folds of the polypeptide and are located in close proximity (dimer formation).

4. Langmuir-Blodgett Films

Chl **b** was investigated in several types of monomolecular Langmuir-Blodgett (LB) films on highly oriented pyrolytic graphite (HOPG) by Clarke and Hanlon.[90,91] They used condensed Chl **b** monolayers (a), Chl **b** monolayers diluted with *cis*-9-octadecen-1-ol (olal) (b), and sample types a and b separated from the surface by a transparent spacer film of arachidic acid ($CH_3(CH_2)_{18}COOH$) (c). Magnetic resonance was performed by fluorescence detection and resonance Raman detection. The results are summarized in Table 8.

The influence of the graphite substrate on D and E is negligible. It seems to affect mostly the triplet sublevel decay channels, especially k_x. This leads to an observed ESP very similar to Chl **b** dimers (see above). Since very little work was done on this interesting system, the mechanism by which the ISC is influenced remains unclear.

C. RADICAL PAIRS *IN VITRO*

The forward ET reaction of photosynthesis has been mimicked by artificial model systems quite extensively. For a more recent review, see Reference 92. Radical pairs have been observed in such systems mostly by magnetic field effects on optical properties. Direct EPR detection of the electron spin polarization of radical pairs has been reported, e.g., by Closs et al.[93] on benzophenone and SDS, and by Buckley et al.[94] on $(isopropylketyl)_2$ radical pairs, but not on radical pairs *in vitro* involving Chl molecules. However, the effects of radical pair interaction during ET reactions between chlorophylls and quinones in organic solvents have been tested by chemically induced electron spin polarization (CIDEP).

It is well known that the Chl triplet state serves as a precursor for photoinduced electron transfer between Chl as electron donor and various acceptors[81,95,96] (for references, see Chapter 1.12). Bowman et al.[44] used pyro-Chl **a** and Zn-pyro-Chl **a** as electron donor and neutral duroquinone (DQ) as electron acceptor in pure ethanol as solvent. Using time-resolved Fourier-transform (FT)-ESR, they were able to detect the time evolution of the CIDEP signal of the DQ anion after an initial laser excitation flash. The polarization of the DQ anion reflects the triplet spin polarization of the donor, thus providing the possibility of measuring T_1 of the triplet state. Due to recombination of the produced radicals and the different lifetime of the radical pairs in their singlet and triplet states, additional CIDEP is mixed in, which

TABLE 9
Electron Transfer-Rate Constants (k_{ET}), T_1 Times for the Acceptor Anion (T_1) and the Donor Triplet ($^3T_1$) for Various ET Reactions in Ethanol Solution

Donor	Acceptor	k_{ET} (M^{-1} s^{-1})	T_1 (μs)	$^3T_1$ (μs)	Ref.
Zn-TPP	DQ	11.1×10^8	7.00	0.46	44
Mg-TPP	DQ	6.1×10^8	3.30	0.23	
Zn-pyro-Chl **a**	DQ	1.87×10^8	7.25		
pyro-Chl **a**	DQ	8.84×10^8	8.80		
Chl **a**	NB	2.6×10^6			95
	1,3-DNB	2.0×10^9			
	1,4-DNB	3.6×10^9			
	Aniline	2.0×10^3			
	N-MeA	7.4×10^3			
	N,N-DMea	3.0×10^4			
	TPA	8.5×10^5			
	TMPD	2.7×10^6			
	Pyridine	$<10^3$			
	2,2-bipyridyl	4.5×10^5			
	1,10-Phenanthroline	1.6×10^6			
	Phenazine	1.1×10^7			
Zn-TPP	BQ	1.8×10^9	≈10	≈0.02	97

Note: TPP = tetraphenylporphine; DQ = duroquinone; NB = nitrobenzene; DNB = dinitrobenzene; MeA = methylaniline; DMeA = dimethylaniline; TPA = triphenylamine; TMPD = tetramethylphenylene diamine; BQ = benzoquinone.

changes the purely absorptive or emissive polarization to E/A. The observed spectra were analyzed taking into account the triplet mechanism (TM) and radical pair mechanism (RPM) which yields T_1 of the triplet precursor as well as the DQ anion and the electron transfer-rate constant k_{ET}. The observed data are found in Table 9. They correspond well to similar data obtained by other authors with conventional optical techniques. The discrepancy in T_1 for the Zn TPP triplet between van Willigen et al.[97] and Bowman et al.[44] may actually be due to insufficient analysis by van Willigen et al.[97] With the application of FT-ESR, one has a very sensitive method for obtaining time-resolved spectral information about short-lived intermediates in ET reactions in the time scale of ≥50 ns. This might prove to be an important advance in the spectroscopy of such processes *in vivo* and *in vitro*, and will eventually be applied directly to the study of radical pair states involving chlorophylls.

IV. THE TRIPLET STATE OF PHOTOSYNTHETIC PIGMENTS *IN VIVO*

A. CHARACTERIZATION

The triplet state is first of all characterized by its dipolar splitting D and E and the sublevel population and decay rates. These parameters have been measured for a large number of bacterial RCs,[98-118,120,125,130] and antenna,[25,26,115,121-124,127] and plant photosystem[4,125-143] complexes, some representative examples of which are found in Tables 10 to 12.

1. Fine Structure Parameters

As can be seen by comparing Tables 10A and 1, the zero-field splittings are generally decreased by 20 to 30% from the monomeric values *in vitro*. This is due to the special pair character of the primary donor on which the triplet state resides. However, the fine structure cannot be accurately calculated by assuming a simple exciton model along the lines of

TABLE 10A
Triplet State Parameters of Bacterial RCs

Strain	Prep.	T (K)	|D| (10^{-4} cm^{-1})	|E| (10^{-4} cm^{-1})	Ref.
Rb. sphaeroides R-26	RC	1.2	188.0 ± 0.4	32.0 ± 0.4	98
	BH_4-treated RC	1.2	190.0	31.9	111
Rb. sphaeroides wild-type 2.4.1	Cells	1.4	185.9 ± 0.6	32.4 ± 0.3	99
Rs. rubrum wild type	Cells	1.4	187.9 ± 0.6	32.4 ± 0.3	99
Rs. rubrum S1	Chromatophores	1.2	189.1 ± 0.6	34.0 ± 0.6	113
Rs. rubrum G9	Cells	5	185	34	120
Rc. gelatinosus	Cells	1.4	185.5 ± 0.6	32.3 ± 0.3	99
Rb. capsulatus ATC 23782	Cells	1.4	184.2 ± 0.6	30.3 ± 0.3	99, 117
Rp. palustris	Chromatophores	1.2	187.8 ± 0.6	39.4 ± 0.6	99
Cr. vinosum	Cells	1.4	177.4 ± 0.6	33.7 ± 0.3	99
	RC	1.5	187.5 ± 0.4	33.8 ± 0.4	101
Cf. aurantiacus	RC	1.2	197.7 ± 0.7	47.3 ± 0.7	104
Rp. viridis	Chromatophores	1.2	156.2 ± 0.7	37.8 ± 0.7	112
	RC	1.2	160.3 ± 0.7	39.7 ± 0.7	112
	RC-crystal	1.2	160.3 ± 0.5	40.2 ± 0.5	116
Rp. sulphoviridis	Chromatophores	1.2	157.1 ± 0.6	38.7 ± 0.6	113
Rb. sulphidophilus	Chromatophores	1.2	186.8 ± 0.6	36.0 ± 0.6	
Th. roseopersicina 6311	Chromatophores	1.2	176.5 ± 0.6	34.7 ± 0.6	
Th. pfennigii 911	Chromatophores	1.2	160.8 ± 0.6	45.4 ± 0.6	
Pr. aestuarii 2K	Chromatophores	1.2	208.8 ± 0.6	36.7 ± 0.6	113

Note: D, E = zero-field splitting parameters. Preparations (Prep.): cells = whole cells; RC = reaction centers.

Sternlicht and McConnell.[73] This model was applied to the BChl dimer in bacterial RCs by Clarke et al.[72] in order to determine special pair geometry, resulting in Eulerian angles incompatible with the data from X-ray crystallography.[144] Using the accurate geometric data of Deisenhofer et al.,[144] one can calculate the D-values for the RC of *Rhodopseudomonas (Rp.) viridis* to be around 212 × 10^{-4} (Reference 124) only if excitonic interaction were involved. This value is much closer to the monomeric data than to the observed D. To account for the additional decrease, CT has been invoked in the triplet state of the special pair. As mentioned earlier, Kooyman and Schaafsma[74] have developed the charge-resonance exciton model to obtain geometric data from the magnetic resonance observables of the triplet state of synthetic dimers. This work has been described in detail by Schaafsma[4] and Kooyman.[145] It takes into account states where the excited electron is transferred to the neighboring molecule (BChl $\mathbf{a}^{+\cdot}$, BChl $\mathbf{a}^{-\cdot}$). The wavefunction has to be written as:

$$\psi = c_1 \cdot \{\psi_a^*\psi_b \pm \psi_a\psi_b^*\} + c_2 \cdot \{\psi_a^+\psi_b^- \pm \psi_a^-\psi_b^+\} \quad (8)$$

with $c_1^2 + c_2^2 = 1$ and c_2/c_1 defining the amount of charge-transfer character. Since D of a biradical is usually negative and very small, depending on the separation between the electrons, CT would tend to lower the overall D according to

$$D = c_1^2 D_{exc} + c_2^2 D_{CT} \quad (9)$$

Very recently, ESR experiments were performed on single crystals of *Rhodobacter (Rb.) sphaeroides* R-26 and *Rp. viridis*, correlating the X-ray structure with the triplet fine structure axes.[146] Figure 2 shows the triplet tensor axes in relation to the BChl molecules of the special pair in *Rb. sphaeroides* R-26.

It is striking that in the case of *Rp. viridis*, the triplet axes coincide, within 5° error, with the molecular axes of the L-side monomer (defined by the interconnection of opposing

TABLE 10B
Triplet State Parameters of Bacterial RCs

Strain	Prep.	$p_x:p_y:p_z$	k_x, k_y, k_z (s^{-1})	T_2 (μs)	Ref.
Rb. sphaeroides R-26	RC			1.16 ± 0.05	103
	Cells	0.484:0.445:0.071	9,000 ± 1,000, 8,000 ± 1,000, 1,400 ± 200		109
Rb. sphaeroides, wild type 2.4.1	Cells	45:45:20 ± 20%	10,500 ± 1,000, 10,000 ± 1,000, 1,700 ± 100		99
				0.5 ± 0.1	102
Rs. rubrum wild type	Cells	45:35:20 ± 20%	7,000 ± 500, 6,500 ± 500, 1,300 ± 100		99
Rc. gelatinosus	Chrom			1.7×10^5	130
Cr. vinosum D	Chrom			1.7×10^5	130
Cf. aurantiacus	RC		12,660 ± 750, 14,290 ± 800, 1,690 ± 50		104
Rp. viridis	RC		13,700 ± 900, 16,100 ± 1,300, 2,420 ± 90		112
Pr. aestuarii 2K	RC		6,790 ± 500, 3,920 ± 300, 1,275 ± 100		115

Note: Preparations (Prep.): chrom = chromatophores; cells = whole cells; RC = reaction centers. p_i (i = x, y, z) = sublevel population probabilities; k_i (i = x, y, z) = sublevel decay rates; T_2 = transversal relaxation time.

TABLE 11
Triplet State Parameters of Antenna Pigments

Strain	Preparation	T (K)	Method	|D| (10^{-4} cm^{-1})	|E| (10^{-4} cm^{-1})	Ref.
Pr. aestuarii	LH-BChl **a** complex	1.2	ADMR	209.8 ± 0.7	55.2 ± 0.7	115
Rb. capsulatus	Cells	1.2	FDMR	206.8 ± 0.5	62.2 ± 0.5	121
Ala$^+$pho$^-$				206.5 ± 0.5	57.9 ± 0.5	
				207 ± 0.5	53.9 ± 0.5	
Rb. capsulatus	Chromatophores	1.2	FDMR	209 ± 5%	67 ± 5%	25, 124, 127
Ala$^+$				214 ± 5%	56 ± 5%	
	LH prep.			210 ± 5%	66 ± 5%	122, 124
				219 ± 5%	58 ± 5%	
Rb. sphaeroides	Chromatophores	1.2	FDMR	215.0 ± 0.5	55.9 ± 0.5	123, 124
R-26.1				215.5 ± 0.5	63.0 ± 0.5	
				216.8 ± 0.5	61.0 ± 0.5	
Rb. sphaeroides	Chromatophores	1.2	FDMR	213 ± 5%	66 ± 5%	26, 124
R-26				220 ± 5%	59 ± 5%	

Note: Preparations: cells = whole cells; LH = light harvesting.

TABLE 12A
Triplet State Parameters of Plant Photosynthetic Complexes

Strain	Preparation	|D| (10^{-4} cm^{-1})	|E| (10^{-4} cm^{-1})	Ref.
Spinach	Chloroplasts	284 ± 5	39 ± 5	125
Atriplex hortensis	CP668	311.7	35.5	129
Ch. reinhardtii	Cells	280 ± 4	32 ± 4	131
Barley	PS I particles	282 ± 1%	38 ± 1%	135
Mastigocladus laminosus	PS I particles unreduced	283	40	140
Synechococcus leopoliensis	PS I particles (SDS)	286.9 ± 0.5	41.7 ± 0.5	142
Anacystis nidulans	Cells + DCMU	283	38	143
Porphyridium cruentum	Cells + DCMU	283	37	
Euglena gracilis	Cells + DCMU	297	37	
Chlorella vulgaris	Cells + DCMU	288	38	
Scenedesmus obliquus C-6E	Cells	287 ± 0.5	38 ± 0.5	4

Note: D, E = zero-field splitting parameters; LDS = lithium dodecyl sulfate; SDS = sodium dodecyl sulfate; DCMU = 3-(3,4-dichlorophenyl)-1,1-dimethylurea.

nitrogen atoms in the porphyrin ring), whereas in *Rb. sphaeroides* the triplet is aligned, within 5° error, with the average of the molecular axes of both monomers. Taking into account the known molecular geometry, the CT character of triplet states could readily be estimated to be 13% for *Rb. sphaeroides* R-26 and 23% for *Rp. viridis*.[146] It seems that in *Rb. sphaeroides* the triplet state has to be treated as being supermolecular, with the excitation energy evenly distributed on both pigments. In *Rp. viridis*, this is evidently not the case, raising the question of the cause of this symmetry breaking. An explanation may be found in the slight differences of the ground-state structure of the two special pairs in question. The M-side BChl in *Rp. viridis* seems to be more strongly puckered than the L-side pigment, which would allow the more planar macrocycle to trap the excited state because the conjugation of the p_z-orbitals is more favored, allowing for a more extensive π-system.

In the case of the AT triplet state, the D-values are much more compatible with the zfs data from monomeric BChl *in vitro* (compare Tables 1 and 11), although somewhat reduced by 5 to 10%. The structure of the AT complexes and the geometric arrangement of their

TABLE 12B
Triplet State Parameters of Plant Photosynthetic Complexes from Spinach

Preparation	T (K)	Method	|D| (10^{-4} cm^{-1})	|E| (10^{-4} cm^{-1})	Ref.
Triton PS I	2	FDMR[a]			141
		(650 nm)	319.7	34.9	
		(670 nm)	269.7	41.2	
		(725 nm)	296.0	40.2	
		(670 nm)	296.7284.0	40.2	
		(680 nm)		43.9	
Chloroplasts	20	ESR	284 ± 5	39 ± 5	125
	2	FDMR	279.4 ± 0.7	38.2 ± 0.7	126
PS I, PS II particles	2	FDMR	388 ± 1.5	38.6 ± 0.1	127
			370 ± 1.5	38.6 ± 0.1	
Digitonin PS I particles	11	ESR	278 ± 9	39 ± 9	128
			383 ± 13	40 ± 13	
PS II particles	4.2	ESR	290	40	132
LDS-PS II particles	4.2	ESR	290	44	133
SDS-PS I particles	4.2	ESR	280 ± 5	38 ± 2	134
Triton-PS I particles (TSF I)	1.2	ADMR	281.7 ± 0.7	38.3 ± 0.7	136
Aged triton PS I particles	1.2	ADMR	278.9 ± 0.7	38.3 ± 0.7	
LDS PS I particles	1.2	ADMR	281.7 ± 0.7	38.3 ± 0.7	
Aged LDS PS I particles	1.2	ADMR	278.9 ± 0.7	38.8 ± 0.7	

Note: D, E = zero-field splitting parameters.

[a] The wavelengths in parentheses denote the detection wavelength in the respective FDMR experiments.

pigments is still under debate. Although the strong red shift in their red-most absorption band implies strong interaction between the AT pigments,[77] their fine-structure values do not seem to be affected that much. Whether the exciton picture is applicable to the triplet state or whether more complex interactions (CT, pigment-protein interactions) have to be taken into account is not yet clear. The observation of a BChl protein-complex as a precursor for the biosynthesis of the photosynthetic proteins in whole cells of *Rb. sphaeroides*[86] seems to imply that the protein as a matrix exerts negligible effects on the fine structure of the porphyrin ring (compare Tables 7 and 1). Trying to deduce the geometric arrangement of the dimer in AT complexes solely from triplet data seems to be premature, however. One deals with the same problems that were encountered with the RCs. It can be shown, however, that the AT complexes of different bacteria show at least two slightly different triplet states, differing mostly in their E-value. This seems to be significant in light of the finding that E is very sensitive to the coordination state of the macrocycle.[39] Although the AT-BChl is mostly in its pentacoordinated state (80 to 90% according to Robert et al.[36]), FDMR at 1.2 K reveals some hexacoordinated pigments.

The D- and E-values of PS I and PS II RCs of plant photosynthesis resemble very much the values of monomeric Chl **a**. Judging only from the triplet data, a monomeric pigment could be assumed to be the primary donor in both cases. This does not necessarily have to be so, however, since certain geometric arrangements of the dimer would result in zfs values resembling monomeric ones. In addition, there is always the possibility of triplet energy being trapped on just one monomer of an arrangement that functions as a supermolecule dimer in the singlet excited state, similar to the case in *Rp. viridis* where CT contributions seem to be the only cause for the decrease in D.

Some remarks are needed to clarify the origin of various additional triplet states in plant photosystems, as reported in the literature and partly shown in Tables 12A and B. There are a number of reports of substantially higher D-values[127,128,135,143] between $330 \cdot 10^{-4}$

TABLE 12C
Triplet State Parameters of Plant Photosynthetic Complexes

Strain	Preparation	$p_x:p_y:p_z$	k_x, k_y, k_z (s^{-1})	k_T (s^{-1})	Ref.
Spinach	SDS-PS I particles		1150 ± 350, 1050 ± 350, ≤130	750 ± 250	134
	Triton-PS I particles (TSF I)		990 ± 100, 1010 ± 100, 92 ± 5		136
	Triton PS I particles		1100 ± 10%, 1300 ± 10%, 83 ± 20%	800 ± 20%	137
Atriplex hortensis	CP668			295 ± 15	129
Ch. reinhardtii	Cells	1:0.7:0.2	1800 ± 270, 850 ± 150, 320 ± 50	800 ± 80	131
		1:0.6:0.1	560 ± 90, 300 ± 40, 60 ± 10	300 ± 50	
	PS II particles		930 ± 40, 1088 ± 50, 110 ± 5		139
Synechococcus leopoliensis	SDS-PS I particles		—,—, 60 ± 40	150 ± 50	142

Note: p_i (i = x, y, z) = sublevel population probabilities; k_i (i = x, y, z) = sublevel decay rates; k_T overall triplet decay rate.

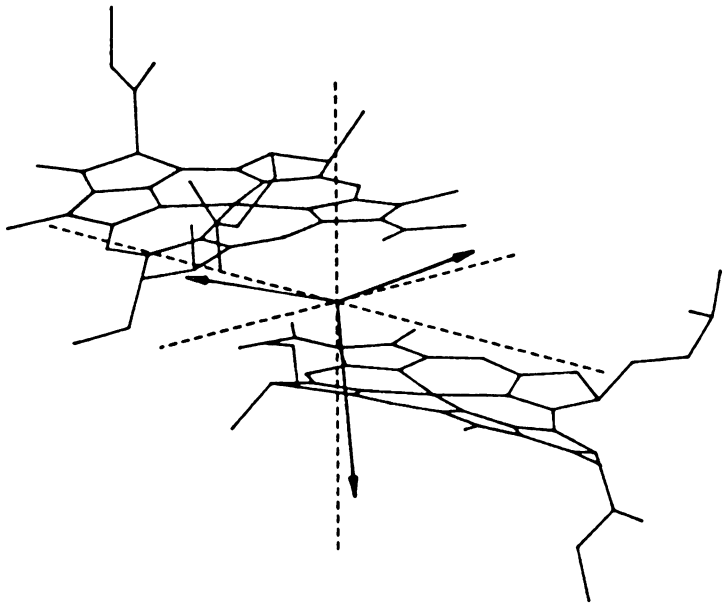

FIGURE 2. Theoretical spin axes for a triplet state that is symmetrically shared between the monomers of the special pair donor (dotted lines) and the experimentally determined directions of the spin axes for the ^3P (arrows) in *Rb. sphaeroides* R-26. Alignment is within 5° for all three axes. The L-monomer BChl is in the lower half of the picture from this perspective. (From Norris, J. R., et al., *Proc. Natl. Acad. Sci. U.S.A.*, 86, 4337, 1989. With permission.)

cm^{-1} and $390 \cdot 10^{-4}$ cm^{-1} associated with a spin-polarization which is not caused by the radical pair mechanism, but, rather, by spin-orbit-mediated ISC.[128] It seems obvious that these resonance lines do not originate from either Chl **a** or Chl **b** species, but, possibly, from carotenoid triplet states whose zfs values lie in that region.[147] D-values between 300 and $340 \cdot 10^{-4}$ cm^{-1} were either ascribed to Chl **b** triplet states forming in the AT complexes[129,135,138,141] or to photooxidized or pheophytinized Chl **a**.[143] Finally, reference should be made to the FDMR work where very narrow 2|E| transitions have been found for *Scenedesmus obliquus* mutant C-6E, *Anacystis nidulans,* and *Chlorella vulgaris*.[4] This was attributed to very narrow τ_x and τ_y levels and selective broadening of the τ_z sublevel, yielding broad |D| + |E| and |D| − |E| signals and narrow 2|E| signals. It seems very strange, however, that this observation has only been made in a number of algal strains, whereas in other strains (e.g., *Scenedesmus* wild type) it was not found. Since it is a very interesting feature, one should try to reproduce this finding with methods different from FDMR, which is well known to pick up even very minute amounts of any fluorescent pigment impurity (e.g., ADMR).

2. Triplet-State Kinetics

The kinetics of the triplet state, i.e., the sublevel decay rates due to spin-selective ISC, the population probabilities depending on the triplet formation mechanism, and the T_1 and T_2 times (spin-lattice and spin-spin relaxation time) have been studied extensively to gain information about pigment-pigment and pigment-protein interaction. It has been pointed out by Hoff and co-workers in a number of papers that the pulse method, developed by van Dorp et al.,[148] is superior to the saturation method used by Clarke et al.,[149,150] mainly because the ideal situation of total saturation of the inhomogeneously broadened ODMR lines of randomly oriented pigments was never reached with the applied microwave power of less

than 1 W.[5,108,109,151] Recent saturation experiments show that saturation is not even achieved with up to 16 W of microwave power.[152] As was shown by Hoff,[5,151] the lower values for the k_x and k_y rates obtained by the saturation method are wrong and have to be corrected by the more accurate pulse method. This has to be kept in mind when comparing the different relaxation rates of Tables 10B and 12C. The saturation method does, however, give the correct result for the slowest relaxation rate, k_z, in accordance with the pulse method. Of course, these rates can also be determined in high field by flash-induced, time-resolved ESR, as shown by Gast and Hoff.[108]

The kinetic decay rates of the triplet sublevels were at first used to determine the geometry of the dimer, using the exciton model.[67,72] Unfortunately, one encounters the same drawbacks as already discussed for the zfs values if CT contributions have to be taken into account. The relative high CT contributions in the RC triplet state may actually be the reason for the comparatively high k_x and k_y decay rates in the special pair.

The population probabilities can be measured from changes in the fluorescence (or absorption) on application of resonant microwaves when the decay rates are known, as outlined by Hoff et al.[5,99] p_x, p_y, and p_z are very close (see Table 10B), which underscores the fact that the triplet state is formed by the radical pair mechanism rather than by normal ISC. A more detailed explanation for the differences between the p_i ($i = x, y, z$) relies on the knowledge of the zero-field splitting tensor of the radical pair triplet state out of which the primary donor triplet state is formed as well as on a proper model for the anisotropic hyperfine interactions in the radical pair. Recent advances in understanding the recombination process in high magnetic fields seem to open the way for such a formulation for the dynamics in zero field.

The spin-spin relaxation time has been studied by both hole-burning experiments[109,116,124,153,154] and spin-echo experiments.[102,103] The homogeneous linewidth of 0.5 to 0.6 MHz derived from the hole-burning data are in good agreement with the spin-echo data of Nishi et al.,[102] yielding a T_2 of 0.5 μs. A more recent ESE study performed on RCs of *Rb. sphaeroides* R-26 produced a somewhat longer T_2 of 1.16 ± 0.05 μs which was temperature independent between 1.2 and 2.1 K.[103] The difference between these ESE data and the hole-burning results is not yet understood. The temperature dependence of T_2 is interesting because it might provide the means of measuring the coupling energy between the two pigments in the special pair, provided that there is a temperature-activated population of the upper Davydov component which would be reflected by the shortening of T_2 together with a possible change in the zfs values (see the following section).[5,103] This is, however, true only if vibronic excitations can be neglected in the range below ≈200 cm^{-1}.

B. TEMPERATURE DEPENDENCE

The temperature dependence of |D| of the RC triplet state was first observed by Hoff and Proskuryakov.[155,156] Using a direct-detection flash ESR technique, they were able to detect the polarized RC triplet state of *Rb. sphaeroides* R-26 and wild type up to room temperature. The most significant result is that the zfs parameter |D| increases by about 7% over the whole temperature range. This finding was interpreted by the authors as excluding the possible temperature-activated admixture of a higher lying CT state, as was proposed by Shuvalov and Parson.[27] Rather, it was explained by an admixture of the triplet state of one of the accessory monomeric BChl molecules[156] or a higher lying vibronic mode of the RC triplet.[155] Frank et al.[157] invoked the first possibility to explain triplet transfer from BChl to carotenoid. Additional information from temperature-dependent triplet-minus-singlet (T-S) spectra[158-160] also indicates no trace of an admixed CT state in the optical spectra of the triplet state. Using the high-resolution ADMR technique in zero field, Ullrich et al.[161,162] were able to substantiate the temperature dependence of the RC zfs parameters, finding a significant increase in D at temperatures above 80 K (see Figure 3). Using the model of

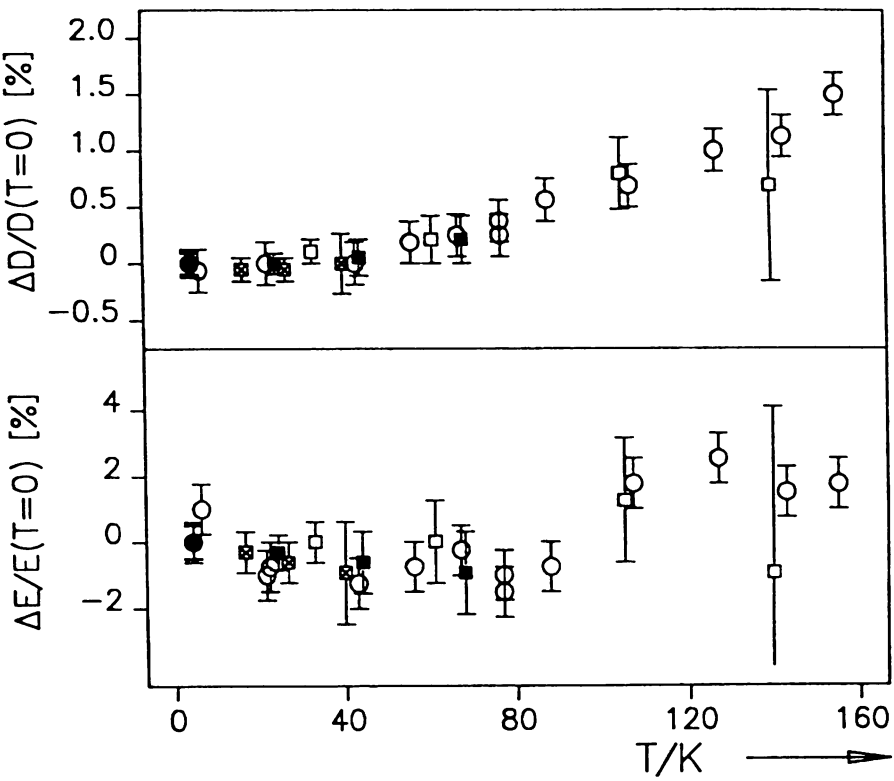

FIGURE 3. Temperature dependence of the zero-field splitting parameters D and E of the RC triplet state in *Rb. sphaeroides* strain R-26 (□), strain GA (■), strain 2.4.1 (⊠), and in *Rp. viridis* (○) from Ullrich.[162] The relative change of D and E versus the value at 4.2 K is plotted over temperature.

Botter et al.,[163] Ullrich derived the zfs parameters and energy gap between the RC triplet of *Rp. viridis* and an apparent higher-lying state T* which may be populated at elevated temperatures[162] (see Figure 4). He found slightly higher zfs values $|D|^* = (165 \pm 1.5) \cdot 10^{-4}$ cm^{-1} and $|E|^* = (41 \pm 0.6) \cdot 10^{-4}$ cm^{-1}, compared to the low-temperature values $|D| = (159.4 \pm 0.2) \cdot 10^{-4}$ cm^{-1} and $|E| = (39.5 \pm 0.2) \cdot 10^{-4}$ cm^{-1}, and an energy gap of 16 ± 3 meV, which is somewhat lower than the number given by Proskuryakov and Manikowski (20 to 30 meV) from their high-field data.[156] Although these data seem to indicate that there is a higher lying triplet state that can be populated from the special pair triplet, one can only speculate about its nature at this time.

Additional evidence for the existence of a triplet state that is accessible by a temperature-activated population from the special pair triplet P^R comes from the temperature dependence of the spin lattice relaxation (SLR) rates. They were measured for RCs of *Rp. viridis* by time-resolved, high-field EPR.[164] The temperature dependence of the SLR rate is quadratic in T below 40 K and remains constant at a level of 13,000 s^{-1} between 40 and 120 K. The same qualitative behavior was observed by Ullrich by extracting the SLR out of the temperature dependence of the signal intensities of his ADMR spectra.[162] One possible explanation for this behavior is that the increase in relaxation below 40 K reflects the relaxation in a triplet state that feeds into P^R. Above 40 K, this state is completely relaxed, thus not affecting the spin polarization any more. This does not necessarily mean that P^R is in Boltzmann equilibrium, since the projection of the spin axes from a fully relaxed precursor state can still result in appreciable spin polarization, depending on the geometry of both states. In fact, the results of Ullrich indicate that P^R is not in equilibrium, even at the highest

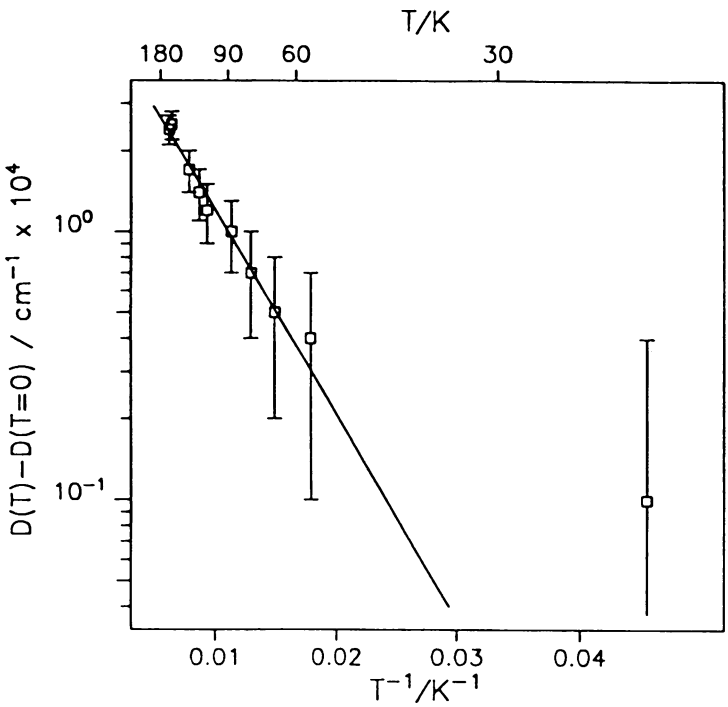

A

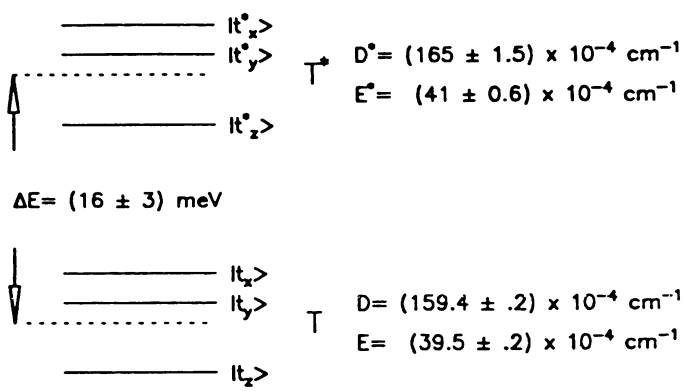

B

FIGURE 4. (A) Arrhenius plot of the difference of D from its value at 4.2 K over the inverse temperature for the RCs of *Rp. viridis*. The rectangles mark the measured values with their respective error bars. The straight line is a least-square fit yielding an activation energy of 16 meV.[162] (B) Proposed energy level scheme for the triplet state in *Rp. viridis* based on the model of temperature-activated population of a higher triplet state to explain the temperature dependence of D (see text for details).[162]

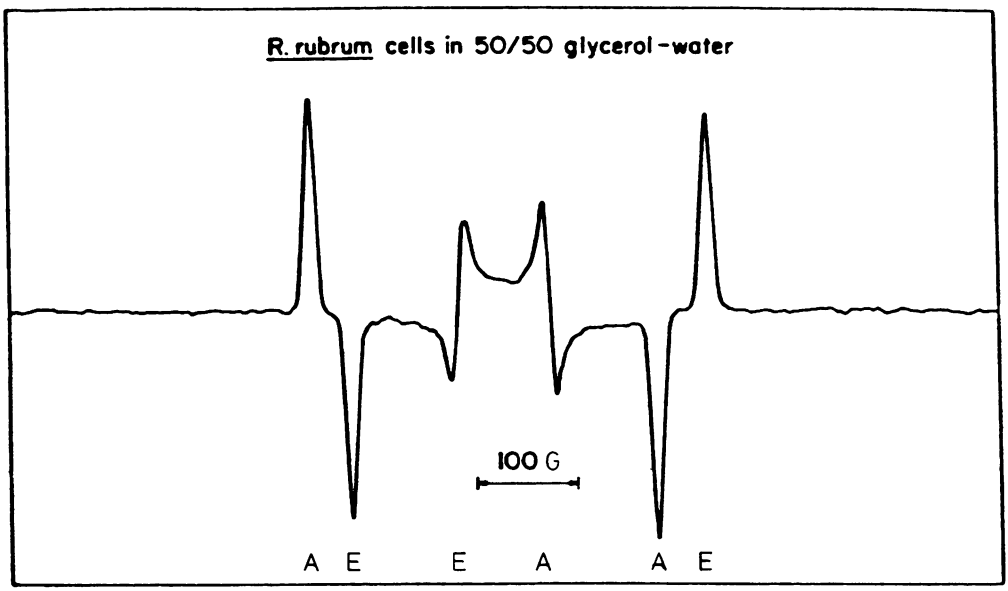

FIGURE 5. Triplet EPR spectrum of whole cells of *Rs. rubrum* in 50:50 glycerol/water mixture at 5 to 20 K. (From Uphaus, R. A., Norris, J. R., and Katz, J. J., *Biochem. Biophys. Res. Commun.*, 61, 1061, 1974. With permission.)

temperatures where he was able to see signals (240 K for *Rp. viridis* and 150 K for *Rb. sphaeroides*).[162] SLR rates were considerably higher in *Rb. sphaeroides*, than in *Rp. viridis*. Speer found a rate of 5000 s^{-1} at 35 K for *Rb. sphaeroides* R-26,[152] whereas, at 133 K and 233 K, Hoff et al.[155] found rates of 290,000 and 400,000 s^{-1} for the relaxation of the Y-peak of the high-field powder spectrum of the triplet state.

C. SPIN POLARIZATION

The photoexcited triplet state of all RCs investigated so far, including plant photosystems I and II, green bacteria, and even crystallized RCs,[165] exhibits a characteristic spin polarization pattern AEEAAE (A = enhanced absorption, E = stimulated emission) very much different from what is normally observed in triplet states generated via an intramolecular ISC mechanism (see Figure 5). This unusual behavior can be explained by the action of the RPM.

The radical pair is created from the singlet state with total magnetization of S = 0. Angular momentum conservation and spin dephasing during the lifetime of the radical pair leads to the preferred population of the m = 0 level of the triplet state, resulting in enhanced absorption for the $|T_0> \rightarrow |T_{+1}>$ transition and emission from the $|T_0> \rightarrow |T_{-1}>$ transition.[125] As Ponte-Goncalves and Spendel[166] pointed out, however, unusual spin polarization patterns resembling those found in the RC triplet state can originate from intramolecular ISC as well and care has to be taken to measure the high-field triplet-level decay rates in order to distinguish them from the RPM. Work on the ESP of the triplet state has been reviewed quite extensively,[1,3-6] so it suffices to mention only some recent studies of RC triplet states.

In earlier work on ESP of the triplet state, the effects of additional electronic spins on the reduced quinones have not been taken into account. These additional spins in the RC are expected to interact with each other, though the interaction (exchange and dipolar coupling) might be weak. For instance, shoulders on the EPR signal of the reduced ubiquinone having a lifetime essentially equal to that of the triplet state were interpreted as originating from the combined effect of exchange and dipolar interaction between the reduced quinone

and the primary donor triplet.[167] The effect of the prereduced quinone on the triplet spin can be seen in the temperature-dependent inversion of ESP in RCs of *Rp. viridis* and chromatophores of *Chromatium vinosum*. At 19 ± 3 K, the central two EPR powder lines invert their polarization, changing the pattern from AEEAAE to AEAEAE.[168] By doubly reducing the quinone acceptor, this effect can be quenched.[169] Although the effect of inversion of the Y-population could not be observed in *Rb. sphaeroides*, perhaps due to a lower exchange interaction of I^- and Q^-, the amplitudes of the Y-peak were significantly affected by replacing the ubiquinone with menaquinone (thereby increasing the exchange interaction).[170] Using time-resolved EPR, van Wijk and Schaafsma[164,171] were able to distinguish the initial ESP from the steady state polarization pattern during the first microseconds after an initial laser flash, when the radical pair state has already recombined but the effect of SLR has not yet kicked in. At 100 K, however, it exhibits an -EAEA- pattern, where "-" means no observable signal at the Z-peaks. A satisfying qualitative explanation was given by Hore et al.,[172] developing a rather simple three-spin model of the reaction center. They treated the magnetic moment of the quinone Fe^{2+} complex as a third spin, acting very much like a nuclear spin in S-T mixing of the radical pair, only with a much larger exchange interaction between the spin on the quinone and the spin on the intermediary acceptor (on the order of 20 mT). Modeling all anisotropic interactions with an anisotropic g of the quinone and introducing SLR for its electron spin, it was possible to theoretically reproduce the observed effects of temperature- and time-dependent polarization inversion. To put it in terms that can be understood more easily: a spin-flip of the quinone, induced by SLR during the lifetime of the triplet radical pair P^+I^-, will cause a concomitant spin-flip on the intermediary acceptor I^-, resulting in an additional population of $T_{\pm 1}$, which tends to reduce the effect of RPM on the ESP of the resulting triplet state ^3P (see Figure 6).

D. TRIPLET-STATE OPTICAL SPECTRA

Triplet-triplet (T-T) absorption spectra of chlorophylls in organic solutions have been studied since the late 1950s. Their common features are a strong band just to the red of the main Soret peak and a broad, sometimes structured plateau in the visible range which decreases in the NIR.[173-175] More recent investigations by Setif et al. demonstrate another broad and very weak band at 1150 nm for Chl **a** *in vitro*.[176] This was also seen in the light-induced absorption difference spectra of PS I-enriched preparations.[177]

During the last few years, Hoff and co-workers in Leiden developed a highly sensitive method to record MIA difference spectra using an ADMR set-up. Using this method and extensions of it, they were able to characterize the optical spectra of the chlorophyll triplet states of a wide variety of bacterial RC and AT as well as the plant photosystems. (See References 98, 101, 104, 112, 113, 115, 136, 139, 158 to 160, 166, 178, 179, and 183 to 195.)

MIA is a very sensitive method for distinguishing T-S spectra of different molecular species (e.g., monomers vs. dimers) which gives information about the pigment that carries the triplet state. Since it not only shows triplet-triplet absorption, but also the corresponding singlet-singlet absorption as well as any breaking of the molecular interaction caused by the formation of the triplet state, it is a very powerful tool for deducing information about the optical transition moments and interactions between the pigment array of the RC. By using polarized techniques (i.e., linear dichroism [LD]-ADMR, a magnetophotoselection application of ADMR), one can even obtain angular information about the arrangement of optical and magnetic transition moments relative to each other. Using *m*agneto*o*ptical absorption *d*ifference *s*pectroscopy (MODS), it was possible to extend the applicable temperature range from below 10 K to room temperature. It is beyond the scope of this chapter to report every detail of MIA applied to photosynthetic complexes. For an updated account of its capabilities and accomplishments, the reader is referred to the excellent Ph.D. thesis by Lous.[178] In the

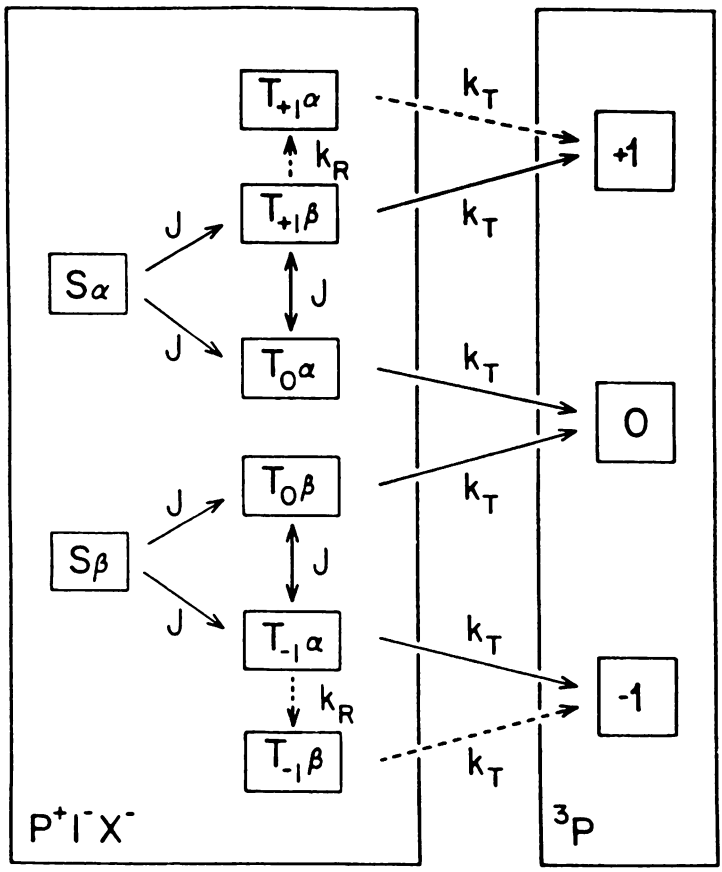

FIGURE 6. The important pathways involved in the reactions $^1[P^+I^-]X^- \rightarrow {}^3[P^+I^-]X^- \rightarrow {}^3PIX^-$. The steps indicated by dashed arrows are only important when X^- undergoes rapid spin-lattice relaxation. The three types of interconversion are labeled as follows: J, coherent mixing mediated principally by $J(I^-X^-)$; k_R, spin-lattice relaxation of X^-; k_T, electron-hole recombination of P^+I^-. (From Hore, P. J. et al., *Biochim. Biophys. Acta*, 936, 255, 1988. With permission of Elsevier Science Publishers B.V.)

following discussion, only a few examples that seem to be the most important results of this kind of spectroscopy of the photosynthetic RCs are given.

Figure 7 shows both the T-S and LD-(T-S) spectra of RCs of *Rp. viridis* at 1.2 K, together with a theoretical simulation based on a simple exciton model of the RC pigments.[178,179] The spectral features between 800 and 870 nm (three positive and two negative peaks in the T-S spectrum) can be explained by the triplet state localized on the L-molecule of the special pair, leaving three exciton-coupled BChls that give rise to this part of the T-S spectrum. The long wavelength band belongs to the lower exciton band of the primary donor. The result for the angle between the optical transition moment of the special-pair pigment $BChl_{LP}$ and the y-axis of the triplet tensor is 10° which compares very well, within error limits, with the single-crystal ESR results of Norris et al.,[146] who found an angle of about 5° between the y-triplet axes of the triplet state localized on $BChl_{LP}$ and the crystallographic y-axis of that pigment. Similar exciton calculations, with basically similar results, were performed by Fischer and his group who also discuss the possibility of CT contributions.[180-182] The latter, however, do not play a major role in the absorption spectra, presumably because of their expected very large bandwidth and low oscillator strength. It should be

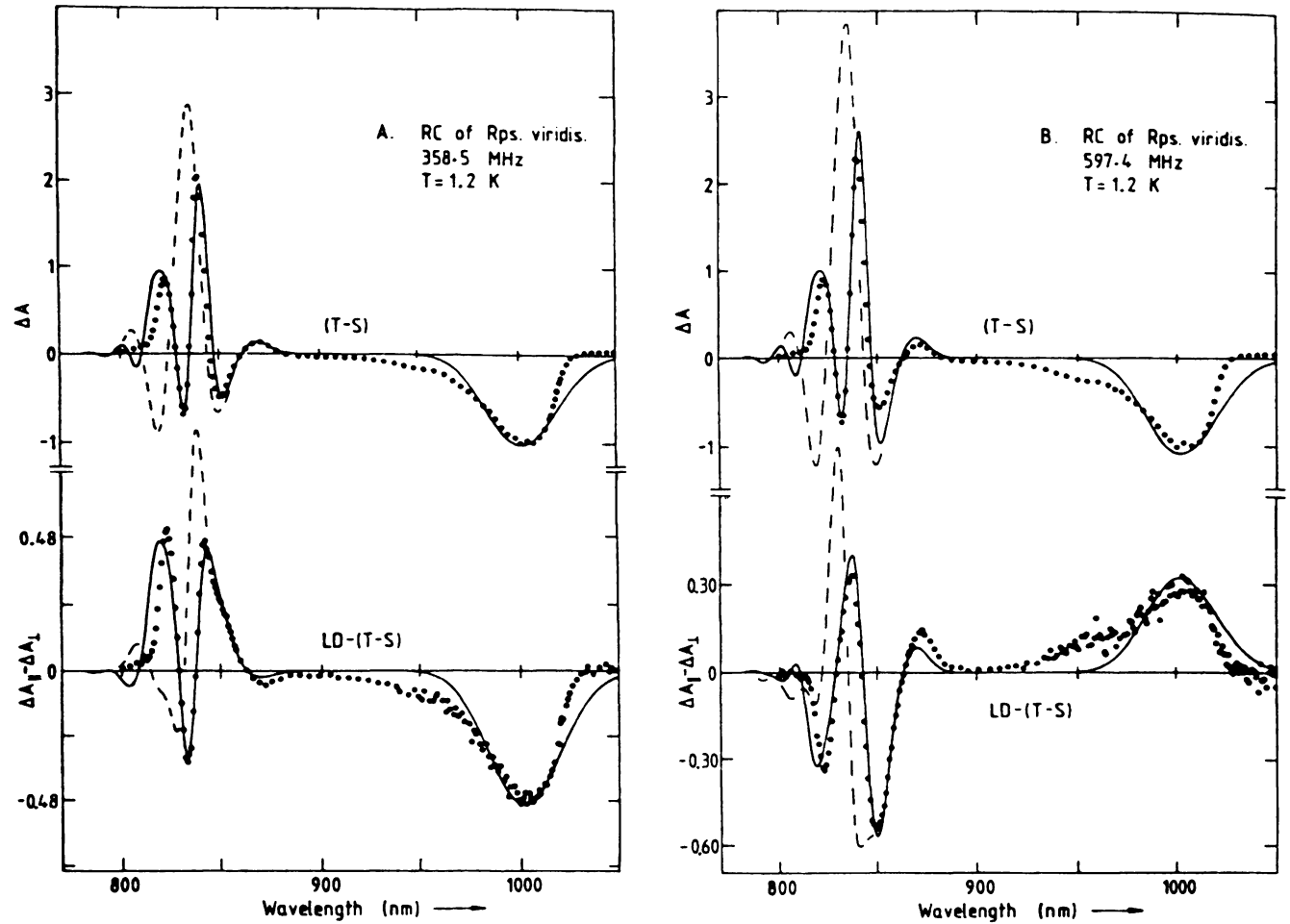

FIGURE 7. (T-S) and LD-(T-S) spectra of RCs of *Rp. viridis* at 1.2 K. ····, Measured spectra; — and - - -, simulated spectra for ^{3}P localized on $BChl_{LP}$ and $BChl_{MP}$, respectively. (From Lous, E. J. and Hoff, A. J., *Proc. Natl. Acad. Sci. U.S.A.*, 84, 6149, 1987. With permission.)

TABLE 13
Best-Fit Parameters Used by Lous et al.[179] for the Fit of the Temperature Dependence of [^{3}Car]/[^{3}P870] from MODS Spectra for *Rb. sphaeroides* 2.4.1 and *Rs. rubrum* S1 Using $k_3 = 7.7 \times 10^4\ s^{-1}$

	Rb. sphaeroides 2.4.1	*Rs. rubrum* S1
$k_1^0\ (s^{-1})$	1.7×10^7	1.2×10^6
$k_2^0\ (s^{-1})$	4.3×10^6	1.6×10^7
ΔH_a (eV)	0.022	0.020
ΔH (eV)	0.155	0.060

mentioned that Scherer and Fischer's model[181] for *Rb. sphaeroides* R-26 was able to adequately explain the MIA spectrum as well as the absorption and CD spectra of borohydride-treated RCs of the same strain, where the $BChl_{MA}$ is thought to be removed.[111,182]

A recent application of the MODS technique is the temperature-dependent study of the triplet energy transfer from the primary donor to the carotenoid (Car) present in all wild-type strains.[160] Using MODS, the T-S spectra of *Rb. sphaeroides* 2.4.1 and *Rs. rubrum* S1 were measured between 10 and 288 K. The relative triplet concentration of the primary donor and carotenoid triplets were calculated from the intensities of the carotenoid triplet-triplet absorption and the primary donor ground-state absorption bands. The temperature dependence of [^{3}Car]/[^{3}P870] was then used on the basis of a simple energy transfer model

$$^3P870 + {}^1Car \underset{k_2}{\overset{k_1}{\rightleftharpoons}} {}^1P870 + {}^3Car \xrightarrow{k_3} {}^1P870 + {}^1Car \tag{10}$$

to determine the forward and backward rates as well as their energy barriers for triplet energy transfer. k_1 and k_2 are the forward and backward rates for triplet transfer respectively, and k_3 is the decay rate for the Car triplet state. k_1 and k_2 are assumed to be temperature dependent, with activation enthalpy ΔH_a and ΔH, respectively, whereas k_3 is temperature independent.

$$k_1 = k_1^0 \cdot \exp^{[-\Delta H_a/kT]} \tag{11a}$$

$$k_2 = k_2^0 \cdot \exp^{[-(\Delta H_a + \Delta H)/kT]} \tag{11b}$$

A four-parameter best fit yielded the results shown in Table 13. It is interesting that in both cases there seems to be the same energy barrier of around 0.02 eV ($\sim$160 cm^{-1}). Whether this energy barrier indicates an intermediate triplet state, possibly the upper Davydov component of ^{3}P870, a vibronically excited form of ^{3}P870, or an excited monomer triplet state $^3BChl_{MA}$, has not been determined yet. However, the finding of such a barrier compares well with the activation energy that was found for the temperature-activated changes in zfs splittings of the primary donor (see Section IV.B) and thus lends additional support to a higher lying triplet state.

As a final example of the application of ADMR, attention is focused on a recent attempt to use zfs values as well as the (T-S) and LD-(T-S) spectra as a taxonomic tool to distinguish between different groups of bacteria.[113] The RCs of a number of Rhodospirillaceae, Chromatiaceae, Chlorobiaceae, and Chloroflexaceae are grouped into three different classes showing different spectral changes, especially in the 800- to 870-nm region of the (T-S) spectra. Class I is characterized by a strong band appearing in the center of that region, flanked by a bandshift at higher energies and a negative and positive band at lower energy.

TABLE 14
Hyperfine Coupling Constants in MHz for the Triplet State of RCs of *Rb. sphaeroides* R-26 (proton couplings) and *Rb. sphaeroides* 2.4.1 (^{15}N couplings)

	α-Protons	β-Protons	Methyl protons	Nitrogen
hfi A	−0.3	2.7	0.45	1.42
(MHz)	−1.4	4.5		1.75
	−2.8			2.04

Note: The proton hfi has only been measured on the Z-peaks of the powder EPR spectra.[186] The nitrogen hfi was the result of an ESEEM study on ^{15}N-enriched RCs.[187,188]

It contains *Rp. viridis, Rp. sulfoviridis, Rb. sulfidophilus, Cr. vinosum* D, *Thiocapsa (Th.) roseopersicina* 6311, *Th. pfennigii* 9111, and *Chloroflexus aurantiacus* J-10-fl. In class II, the same central band appears to be much weaker (compared with the special-pair band at lower energies), the bandshift at higher energies is much less pronounced, and the intensity of the two bands at lower energy is almost entirely in the positive band. It contains *Rp. palustris, Rs. rubrum* S1, *Rb. sphaeroides* R-26, *Rb. sphaeroides* 2.4.1, and *Rb. capsulatus* 23782. In class III, the features at 820 nm are overlapped by a special pair much closer to this region than in the other classes. This is the class of the green photosynthetic bacteria, of which only *Pr. aestuarii* 2K has been investigated so far. A simple explanation for these different features seems to come from the simulation of the spectra. In class I, the triplet state is localized on the $BChl_{LP}$ monomer of the special pair, whereas in class II the triplet state seems to be at least partly delocalized (the probability of localization is less than 70%) between both parts of the special pair. A description of class III cannot be given because of the lack of an adequate exciton model. Whether this classification will prove to be a meaningful taxonomic tool is yet uncertain. Many more strains will have to be examined to determine its significance. The changes in the spectral features are sufficiently pronounced, however, to provoke thought about possible underlying differences.

E. HYPERFINE STRUCTURE

The nuclear hyperfine structure of the triplet state has been investigated by both ENDOR[186] and ESE envelope-modulation (ESEEM)[187,188] spectroscopy. The data sets of both experiments complement each other, since the ENDOR experiment was done only at the proton resonance frequencies and the ESEEM yielded only the low-frequency nitrogen hyperfine (hf) and nuclear quadrupole couplings. Table 14 presents the hyperfine couplings for both protons and ^{15}N nuclei.

From comparisons of proton hyperfine data of the primary donor cation and nitrogen hyperfine couplings of monomeric BChl anion and cation radicals, Lendzian et al.[186] and de Groot et al.[187] conclude that their data reflect a triplet state shared by both pigments of the special pair on the EPR timescale, a result which was confirmed by the single-crystal work of Norris et al.[146]

V. RADICAL PAIRS IN PHOTOSYNTHETIC REACTION CENTERS

As already outlined in Section I, radical pairs form during the primary-charge transfer step in photosynthetic RCs. The most successful methods applied to its study so far have been RYDMR (*r*eaction *y*ield-*d*etected *m*agnetic *r*esonance), where the triplet yield is used to monitor transitions in the radical pair, MARY (*ma*gnetic field effect of *r*eaction *y*ield),

where the triplet yield is monitored as a function of a magnetic field applied to the sample, and ESP (*e*lectron *s*pin *p*olarization) of CIDEP (*c*hemically *i*nduced *d*ynamic *e*lectron-spin *p*olarization), where the spin polarization of the products of the electron-transfer reaction, i.e., the oxidized primary donor and the reduced quinone acceptor, is analyzed in order to obtain information about the history of its formation. The reader is referred to the review by Hoff[17] for information about the research done in this field through 1986.

A. THEORETICAL MODELS

Determination of the characteristics of the radical pair P^+BH^-, i.e., the exchange interaction J, dipolar splitting parameters D and E, decay rates for singlet and triplet recombination k_S and k_T, is important for the overall description of the primary charge separation in photosynthesis.

Any theory which describes the forward reaction has to be compatible with the experimental findings for the backreaction. Detailed discussions of the various models for the primary electron transfer process[189-200] that are currently traded with regard to the magnetic interactions of the unpaired spins can be found in several publications by Michel-Beyerle and Jortner.[201-204] In these reports, the superexchange mechanism was favored over the sequential mechanism (involving P^+B^-H) mainly because J and k_T turned out to be almost independent of temperature. The very recent experimental observation of a BChl anion in the forward reaction by Holzapfel et al.,[205] however, would seem to justify reconsidering all experimental observations in order to develop a coherent model for the sequential mechanism of ET.

B. PARAMETERS OF THE RADICAL PAIR

Since the experimental methods used in investigating the radical-pair state have been covered by the review of Hoff,[17] this section proceeds directly to the results of these measurements. The reader is reminded, however, that the radical pair has not been observed directly by magnetic resonance, due to its short lifetime. Using rather indirect methods like CIDEP, MARY, or RYDMR, one must rely on fitting the experimental observations to theoretical models in order to extract the desired parameters. In the following discussion, the energy level and kinetic scheme of Ogrodnik et al.[206] (see Figure 8) is used to illustrate the different parameters of the RP, which are listed in Table 15.

Although there seems to be substantial variability in the various parameters listed, experiments and theory have converged on what is widely considered to be the best parameter set, which puts |J| to about 7 to 8 G with little variation with temperature, D at about the same value, k_T at around $5 \times 10^8\ s^{-8}$, and k_S at around $4 \times 10^7\ s^{-1}$.

The sign of the exchange interaction has not yet been determined unambiguously. In the usual notation,[218] J becomes negative when the energy of the singlet state is lower than that of the corresponding triplet state. Positive J (in the above notation) has been proposed on the basis of RYDMR results.[211,220,221] Negative J, however, was favored from the results of ESP lineshape analysis.[222,223]

In order to reduce the ambiguity of the theoretical fits to the observed ESP, Feezel et al.[218] investigated the ESP at Q- and X-band frequencies of iron-depleted RCs whose primary donor P870, intermediate BPhe acceptor, and primary quinone acceptor had been selectively deuterated or protonated. The results showed a definite contribution to the overall ESP by the coupled radical pair having one electron on the primary donor and the other on the quinone acceptor.

In fact, the high-field data could possibly be interpreted by ESP resulting from a spin-correlated radical pair only. Other ESP experiments done at high magnetic fields (K- and Q-band) on plant photosystem I seem to substantiate these findings.[224,225] The problem of how to interpret the measured ESP — by polarization transfer from the intermediate RP P^+I^- to magnetically uncoupled P^+IQ^- or by a magnetically coupled RP P^+IQ^- without

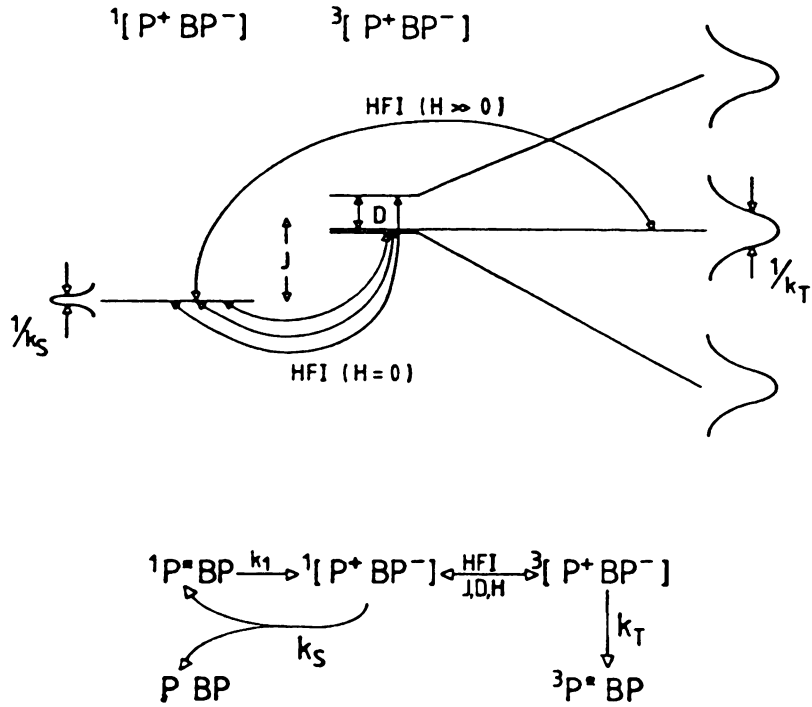

FIGURE 8. Energy levels and kinetic scheme of the radical pair P^+BQ^-. (According to Ogrodnik, A., Rémy-Richter, N., Michel-Beyerle, M. E., and Feick, R., *Chem. Phys. Lett.*, 135, 577, 1987. With permission of Elsevier Science Publishers B.V.)

contribution from P^+I^- — is addressed further by Hore et al.[217] and Stehlik et al.[230] In addition to these two extremes, efforts have been made very recently to reconcile both views and to develop a model for ESP that includes contributions from both radical pairs.[226,227] A complete theoretical analysis of these effects, of course, deals with the difficulty of having to adjust a large number of only partially known parameters to fit the experimental observation.

The recently observed time-resolved ESP spectra of PS I[228-230] will be of great importance for these theoretical models, since they already yield direct information on the ET rates. They also show the anisotropic nature of the measured ESP, which has to be taken into account in future models of the magnetic interaction in the radical pair of photosynthetic RCs. g-Anisotropy for P^+ and Q^-, respectively, have been modeled for the transient ESP in PS I by Stehlik et al.[230]

VI. SUMMARY

Due to the limited space available for this review, the information has been mainly condensed in tables which may be used as a reference to the numerous original articles.

Basic research has been devoted to an understanding of the influence of the environment (pigment-solvent and pigment-pigment interactions) on the characteristic parameters of the Chl triplet state. Although these influences are as yet not fully understood, they supply an empirical basis for the identification and characterization of Chl triplet states *in vivo*. Spectroscopy of the primary donor Chl triplet state in photosynthetic RCs has contributed considerably to the understanding of the optical spectra and the excitonic interactions in these pigment-protein complexes. The occurrence of additional triplet states in RCs has been inferred from different observations (temperature dependence of D, SLR rates, and triplet ESP). The nature of such additional triplet states is, however, still unclear.

TABLE 15
Radical Pair State Parameters Found by Different Experimental Methods in RCs of Photosynthetic Bacteria

Strain	Method	T (K)	|J| (G)	|D| (G)	k_S (s^{-1})	k_T (s^{-1})	Ref.
Rb. sphaeroides R-26	RYDMR	296	≥8, ≤16	5.2	≥4 × 10^7, ≤ 8 × 10^7	≥2 × 10^8, ≤8 × 10^8	215
quinone depl.		296	16 ± 4	50 ± 10	(6.7 ± 1.8) × 10^7	(5.6 ± 0.6) × 10^8	211
		296	15	0	6 × 10^7	5.7 × 10^8	212
	τ_{RP}-RYDMR	100—296	14 ± 1				208
	LF-RYDMR	240—293	≥0.5, ≤5		(4.0 ± 0.2) × 10^8[a]		209
		211	10.1 ± 0.5		(2.6 ± 0.1) × 10^8[a]		210
	B_1-RYDMR, MARY	140—296	14 ± 2	<21	4 × 10^7	5 × 10^8	216
	MARY	90—295	≤15			6 × 10^8	216
	ESP	6	0	1.4			217
Rb. sphaeroides R-26	ADMR	10	≤17	8.6	1.2 × 10^8[a]		214
	LF-RYDMR	240—293	≥0.5, ≤5		(4.2 ± 0.2) × 10^8[a]		209
		211	10.1 ± 0.3		(2.6 ± 0.1) × 10^8[a]		210
		236	9.3 ± 0.2		(2.3 ± 0.4) × 10^8[a]		
		268	8.0 ± 0.1		(3.2 ± 0.1) × 10^8[a]		
		279	7.0 ± 0.1		(3.8 ± 0.2) × 10^8[a]		
		281	5.2 ± 0.1		(3.7 ± 0.2) × 10^8[a]		
		293	3.3 ± 0.1		(3.0 ± 0.2) × 10^8[a]		
	B_1-RYDMR	296	14		3.7 × 10^7	(5.0 ± 0.2) × 10^8	207
Rb. sphaeroides wild type	B_1-RYDMR	296	14		3.7 × 10^7	(4.3 ± 0.2) × 10^8	
Rp. viridis	Calculated			11			213
				5.2			215

Note: The parameters are listed following the notation used in Figure 8. B_1-RYDMR = B_1 field dependence of the RYDMR signal; τ_{RP}-RYDMR = radical-pair decay time-monitored RYDMR; LF-RYDMR = low-field RYDMR; J = exchange interaction of P^+I^-; D = dipolar interaction of P^+I^-, k_S = singlet radical pair $^1[P^+I^-]$ decay rate; k_T = triplet radical pair $^3[P^+I^-]$ decay rate.

[a] Data determined for $k_S + k_T$.

The parameters of the radical pair state P^+BH^- in photosynthetic RCs have been probed and agreement seems to have been reached on the basic values of $|J|$, D, and the decay rates k_S and k_T. Knowledge of these parameter has direct significance for the understanding of the primary forward-charge separation.

REFERENCES

1. **Levanon, H. and Norris, J. R.,** The photoexcited triplet state and photosynthesis, *Chem. Rev.*, 78, 185, 1978.
2. **Thurnauer, M. C.,** ESR study of the photoexcited triplet state in photosynthetic bacteria, *Rev. Chem. Int.*, 3, 197, 1979.
3. **Hoff, A. J.,** Applications of ESR in photosynthesis, *Phys. Rep.*, 54, 75, 1979.
4. **Schaafsma, T. J.,** ODMR spectroscopy in photosynthesis I. The chlorophyll triplet state in vitro and in vivo, in *Triplet State ODMR Spectroscopy*, Clarke, R. H., Ed., John Wiley & Sons, New York, 1982, 291.
5. **Hoff, A. J.,** ODMR spectroscopy in photosynthesis II. The reaction center triplet in bacterial photosynthesis, in *Triplet State ODMR Spectroscopy*, Clarke, R. H., Ed., John Wiley & Sons, New York, 1982, 367.
6. **Hoff, A. J.,** Electron spin polarization of photosynthetic reactants, *Q. Rev. Biophys.*, 17, 153, 1984.
7. **Hoff, A. J.,** Electron paramagnetic resonance in photosynthesis, in *Photosynthesis*, Amesz, J., Ed., Elsevier, Amsterdam, 1987, 97.
8. **Möbius, K. and Lubitz, W.,** in ENDOR spectroscopy in photobiology and biochemistry, *Biological Magnetic Resonance*, Vol. 7, Berliner, L. J. and Reuben, J., Eds., Plenum Press, New York, 1987, 129.
9. **Möbius, K.,** Multiple resonances involving electron spin resonance, nuclear magnetic resonance, and optical transitions: more than just a game?, *J. Chem. Soc. Faraday Trans. 1*, 83, 3469, 1987.
10. **Levanon, H.,** Spin polarized triplets oriented in liquid crystals, *Rev. Chem. Int.*, 8, 287, 1987.
11. **Clarke, R. H., Hobart, D. R., and Leenstra, W. R.,** Investigation of the structure of the reaction center chlorophyll complex by optical detection of triplet state magnetic resonance, *Semicond. Insul.*, 4, 313, 1978.
12. **Grätzel, M.,** Artificial photosynthesis, energy- and light-driven electron transfer in organized molecular assemblies and colloidal semiconductors, *Biochim. Biophys. Acta*, 683, 221, 1982.
13. **Crofts, A. R. and Wraight, C. A.,** The electrochemical domain of photosynthesis, *Biochim. Biophys. Acta*, 726, 149, 1983.
14. **Boxer, S. G.,** Model reactions in photosynthesis, *Biochim. Biophys. Acta*, 726, 265, 1983.
15. **Marcus, R. A. and Sutin, N.,** Electron transfer in chemistry and biology, *Biochim. Biophys. Acta*, 811, 265, 1985.
16. **Khairutdinov, R. F. and Brickenstein, E. Kh.,** Long range electron tunneling in biological and model systems, *Photochem. Photobiol.*, 43, 339, 1986.
17. **Hoff, A. J.,** Magnetic interactions between photosynthetic reactants, *Photochem. Photobiol.*, 43, 727, 1986.
18. **Trifunac, A. D., Lawler, R. G., Bartels, D. M., and Thurnauer, M. C.,** Magnetic resonance studies of paramagnetic transients in liquids, *Prog. React. Kinet.*, 14, 43, 1986.
19. **Budil, D. E., Gast, P., Chang, C.-H., Schiffer, M., and Norris, J. R.,** Three-dimensional X-ray crystallography of membrane proteins: insights into electron transfer, *Annu. Rev. Phys. Chem.*, 38, 561, 1987.
20. **Kirmaier, C. and Holten, D.,** Primary photochemistry of reaction centers from the photosynthetic purple bacteria, *Photosynth. Res.*, 13, 225, 1987.
21. **Hanson, L. K.,** Theoretical calculations of photosynthetic pigments, *Photochem. Photobiol.*, 47, 903, 1988.
22. **Parson, W. W. and Ke, B.,** Primary photochemical reactions, in *Photosynthesis*, Govindjee, Ed., Academic Press, New York, 1982, 331.
23. **Boxer, S. G., Chidsey, C. E. D., and Roelofs, M. G.,** Magnetic field effects on reaction yields in the solid state: an example from photosynthetic reaction centers, *Annu. Rev. Phys. Chem.*, 34, 389, 1983.
24. **Thurnauer, M. C. and Budil, D. E.,** The chlorophyll triplet state as a probe of structure and function in photosynthesis, *Biochim. Biophys. Acta*, in preparation.
25. **Angerhofer, A., von Schütz, J. U., and Wolf, H. C.,** Fluorescence-detected magnetic resonance of the antenna bacteriochlorophyll triplet states of the purple photosynthetic bacteria, in *Antennas and Reaction Centers of Photosynthetic Bacteria*, Michel-Beyerle, M. E., Ed., Springer-Verlag, Berlin, 1985, 78.

26. **Angerhofer, A., von Schütz, J. U., and Wolf, H. C.,** Fluorescence detected magnetic resonance studies on photosynthetic bacteria, in *Proc. 5th Int. Semin. Energy Transfer in Condensed Matter,* Pančoška, P. and Pantofliček, J., Eds., Vydala Jednota Československych Matematiku a Fyziku, Prague, 1986, 59.
27. **Shuvalov, V. A. and Parson, W. W.,** Energies and kinetics of radical pairs involving bacteriochlorophyll and bacteriopheophytin in bacterial reaction centers, *Proc. Natl. Acad. Sci. U.S.A.*, 78, 957, 1981.
28. **Thurnauer, M. C., Katz, J. J., and Norris, J. R.,** The triplet state in bacterial photosynthesis: possible mechanisms of the primary photo-act, *Proc. Natl. Acad. Sci. U.S.A.*, 72, 3270, 1975.
29. **Budil, D. E.,** Magnetic Characterization of the Primary Radical Pair State of Bacterial Photosynthesis, Ph.D. thesis, University of Chicago, Chicago, 1986.
30. **Schulten, K. and Wolynes, P. G.,** Semiclassical description of electron spin motion in radicals including the effect of electron hopping, *J. Chem. Phys.*, 68, 3292, 1978.
31. **Rebeiz, C. A. and Bélanger, F. C.,** Chloroplast biogenesis—46. Calculation of net spectral shifts induced by axial ligand coordination in metalated tetrapyrroles, *Spectrochim. Acta Part A,* 40, 793, 1984.
32. **Bélanger, F. C. and Rebeiz, C. A.,** Chloroplast biogenesis—47. Spectroscopic study of net spectral shifts induced by axial ligand coordination in metalated tetrapyrroles, *Spectrochim. Acta Part A,* 40, 807, 1984.
33. **Goedheer, J. C.,** Investigations on bacteriochlorophyll in organic solutions, *Biochim. Biophys. Acta,* 27, 478, 1958.
34. **Evans, T. A. and Katz, J. J.,** Evidence for 5- and 6-coordinated magnesium in bacteriochlorophyll a from visible absorption spectroscopy, *Biochim. Biophys. Acta,* 396, 414, 1975.
35. **Cotton, T. M. and van Duyne, R. P.,** Characterization of bacteriochlorophyll interactions in vitro by resonance Raman spectroscopy, *J. Am. Chem. Soc.*, 103, 6020, 1981.
36. **Robert, B. and Lutz, M.,** Structures of antenna complexes of several rhodspirillales from their resonance Raman spectra, *Biochim. Biophys. Acta,* 807, 10, 1985.
37. **Clarke, R. H., Hotchandani, S., Jagannathan, S. P., and Leblanc, R. M.,** Ligand effects on the triplet state of chlorophyll, *Chem. Phys. Lett.*, 89, 37, 1982.
38. **Hotchandani, S., Clarke, R. H., and Leblanc, R. M.,** Zero-field optical detection of magnetic resonance of chlorophyll b in n-octane, *Can. J. Chem.*, 64, 188, 1986.
39. **Angerhofer, A., von Schütz, J. U., and Wolf, H. C.,** Fluorescence detected magnetic resonance of bacteriochlorophyll in organic solution, *Chem. Phys. Lett.*, 151, 195, 1988.
40. **Clarke, R. H., Hotchandani, S., Jagannathan, S. P., and Leblanc, R. M.,** The effect of coordinating ligands on the triplet state of chlorophyll, *Photochem. Photobiol.*, 36, 575, 1982.
41. **Bowman, M. K.,** Intersystem crossing in photosynthetic pigments, *Chem. Phys. Lett.*, 48, 17, 1977.
42. **Kleibeuker, J. F., Platenkamp, R. J., and Schaafsma, T. J.,** The triplet state of photosynthetic pigments. I. Pheophytins, *Chem. Phys.*, 27, 51, 1978.
43. **Clarke, R. H., Connors, R. E., Schaafsma, T. J., Kleibeuker, J. F., and Platenkamp, R. J.,** The triplet state of chlorophylls, *J. Am. Chem. Soc.*, 98, 3674, 1976.
44. **Bowman, M. K., Toporowicz, M., Norris, J. R., Michalski, T. J., Angerhofer, A., and Levanon, H.,** Fourier transform-EPR spectroscopy of electron transfer from excited state of chlorophyll and porphyrin to duroquinone, *Isr. J. Chem.*, 28, 215, 1988.
45. **Clarke, R. H. and Connors, R. E.,** An investigation of the triplet state dynamics of zinc chlorophyll b by microwave-induced changes in the intensity of fluorescence and singlet-singlet absorption, *Chem. Phys. Lett.*, 33, 365, 1975.
46. **Clarke, R. H. and Frank, H. A.,** Investigation of the effect of metal substitution on the triplet state of chlorophyll by optically detected zero-field magnetic resonance, *Chem. Phys. Lett.*, 51, 13, 1977.
47. **Antheunis, D. A., Schmidt, J., and van der Waals, J. H.,** Spin-forbidden radiationless processes in isoelectronic molecules: anthracene, acridine, and phenazine. A study by microwave induced delayed phosphorescence, *Mol. Phys.*, 27, 1521, 1974.
48. **Metz, F., Friedrich, S., and Hohlneicher, G.,** What is the leading mechanism for the nonradiative decay of the lowest triplet state of aromatic hydrocarbons?, *Chem. Phys. Lett.*, 16, 353, 1972.
49. **Kanamura, N. and Lim, E. C.,** $T_1[\pi,\pi^*] - S_0$ radiationless transitions in aromatic molecules with nonbonding electrons, *J. Chem. Phys.*, 65, 4055, 1976.
50. **Mauring, K., Renge, I., Sarv, P., and Avarmaa, R.,** Fluorescence-detected triplet kinetics study of the specifically solvated chlorophyll a and protochlorophyll in frozen solution, *Spectrochim. Acta Part A,* 43, 507, 1987.
51. **Renge, I. and Avarmaa, R.,** Specific solvation of chlorophyll a: solvent nucleophility, hydrogen bonding and steric effects on absorption spectra, *Photochem. Photobiol.*, 42, 253, 1985.
52. **Gonen, O. and Levanon, H.,** EPR study of oriented photoexcited triplets of zinc porphyrin in a discotic liquid crystal: evidence for axial symmetry in the condensed phase, *J. Chem. Phys.*, 78, 2214, 1983.
53. **Levanon, H.,** Laser photolysis of zinc porphyrin dissolved in cyanohexylbiphenyl liquid crystal, *Chem. Phys. Lett.*, 90, 465, 1982.
54. **Gonen, O. and Levanon, H.,** Line-shape analysis of transient triplet electron paramagnetic resonance spectra. Application to porphyrins and chlorophylls in nematic uniaxial liquid crystals, *J. Phys. Chem.*, 88, 4223, 1984.

55. **Levanon, H. and Norris, J. R.,** Triplet state and chlorophylls, in *Molecular Biology and Biophysics,* Vol. 35, Fong, F. K., Ed., Springer-Verlag, Berlin, 1982, 152.
56. **Fessmann, J., Rösch, N., Ohmes, E., and Kothe, G.,** Molecular dynamics studied by transient ESR mutation spectroscopy of photoexcited triplet states: chlorophyll a in liquid crystalline matrix, *Chem. Phys. Lett.,* 152, 491, 1988.
57. **Fessmann, J.,** Zeitaufgelöste ESR-Messungen an photoangeregtem Chlorophyll a—Relaxation in Flüssigkristalliner Matrix, Ph.D. thesis, Universität Stuttgart, Stuttgart, Germany, 1987.
58. **Norris, J. R., Druyan, M. E., and Katz, J. J.,** Electron nuclear double resonance of bacteriochlorophyll free radical in vitro and in vivo, *J. Am. Chem. Soc.,* 95, 1680, 1975.
59. **Norris, J. R., Uphaus, R. A., Crespi, H. L., and Katz, J. J.,** Electron spin resonance of chlorophyll and the origin of signal I in photosynthesis, *Proc. Natl. Acad. Sci. U.S.A.,* 68, 625, 1971.
60. **Katz, J. J. and Norris, J. R.,** Chlorophyll and light energy transduction in photosynthesis, *Curr. Top. Bioenerg.,* 5, 41, 1973.
61. **Shipman, L. L., Cotton, T. M., Norris, J. R., and Katz, J. J.,** New proposal for structure of special-pair chlorophyll, *Proc. Natl. Acad. Sci. U.S.A.,* 73, 1791, 1976.
62. **Fong, F. K.,** Molecular symmetry and exciton interaction in photosynthetic primary events, *Appl. Phys.,* 6, 151, 1975.
63. **Plato, M., Tränkle, E., Lubitz, W., Lendzian, F., and Möbius, K.,** Molecular orbital investigation of dimer formations of bacteriochlorophyll a. Model configurations for the primary donor of photosynthesis, *Chem. Phys.,* 107, 185, 1986.
64. **Periasamy, N., Linschitz, H., Closs, G. L., and Boxer, S. G.,** Photoprocesses in covalently linked pyrochlorophyllide dimer: triplet state formation and opening and closing of hydroxylic linkages, *Proc. Natl. Acad. Sci. U.S.A.,* 75, 2563, 1978.
65. **Journeaux, R., Chene, G., and Viovy, R.,** Dimérisation de la Chlorophylle dans les solvants apolaires. Étude de l'équilibre et de l'état triplet, *J. Chim. Phys.,* 74, 1203, 1977.
66. **Hoshino, H., Imamura, M., Koike, K., Kikuchi, K., and Kokubun, H.,** Photo-excited triplet state of dimeric chlorophyll a in 3-methylpentane rigid matrix at 77 K studied by flash photolysis, *Photochem. Photobiol.,* 38, 255, 1983.
67. **Clarke, R. H., Hobart, D. R., and Leenstra, W. R.,** The triplet state of the chlorophyll dimer, *J. Am. Chem. Soc.,* 101, 2416, 1979.
68. **Clarke, R. H. and Hobart, D. R.,** Structural aspects of the reaction center of photosynthetic bacteria calculated from triplet state zero-field splittings, *FEBS Lett.,* 82, 155, 1977.
69. **Hägele, W., Schmid, D., and Wolf, H. C.,** Triplet-state electron spin resonance of chlorophyll *a* and *b* molecules and complexes in PMMA and MTHF II: interpretation of the experimental results, *Z. Naturforsch. Teil A,* 33, 94, 1978.
70. **Kooyman, R. P. H., Schaafsma, T. J., and Kleibeuker, J. F.,** Fluorescence spectra and zero-field magnetic resonance of chlorophyll *a*-water complexes, *Photochem. Photobiol.,* 26, 235, 1977.
71. **Kooyman, R. P. H., Schaafsma, T. J., Jansen, G., Clarke, R. H., Hobart, D. R., and Leenstra, W. R.,** A comparative study of dimerisation of chlorophylls and pheophytins by fluorescence and ODMR, *Chem. Phys. Lett.,* 68, 65, 1979.
72. **Clarke, R. H., Connors, R. E., Frank, H. A. and Hoch, J. S.,** Investigation of the structure of the reaction center in photosynthetic systems by optical detection of triplet state magnetic resonance, *Chem. Phys. Lett.,* 45, 523, 1977.
73. **Sternlicht, H. and McConnell, H. M.,** Paramagnetic excitons in molecular crystals, *J. Chem. Phys.,* 35, 1793, 1961.
74. **Kooyman, R. P. H. and Schaafsma, T. J.,** A charge resonance-exciton model of molecular dimers, *J. Mol. Struct.,* 60, 373, 1980.
75. **Norris, J. R., Uphaus, R. A., and Katz, J. J.,** ESR of triplet states of chlorophylls *a*, *b*, c_1, c_2, and bacteriochlorophyll *a*. Applications of ZFS and electron spin polarization to photosynthesis, *Chem. Phys. Lett.,* 31, 157, 1975.
76. **Gottstein, J. and Scheer, H.,** Long-wavelength-absorbing forms of bacteriochlorophyll *a* in solutions of triton X-100, *Proc. Natl. Acad. Sci. U.S.A.,* 80, 2231, 1983.
77. **Scherz, A. and Parson, W. W.,** Oligomers of bacteriochlorophyll and bacteriopheophytin with spectroscopic properties resembling those found in photosynthetic bacteria, *Biochim. Biophys. Acta,* 766, 653, 1984.
78. **Scherz, A. and Parson, W. W.,** Exciton interactions in dimers of bacteriochlorophyll and related molecules, *Biochim. Biophys. Acta,* 766, 666, 1984.
79. **Krasnovsky, A. A. and Semenova, A. N.,** Parameters of the triplet state and spectral properties of the monomeric chlorophyll in liposomes at −196°C, *Photobiochem. Photobiophys.,* 3, 11, 1981.
80. **Ford, W. E. and Tollin, G.,** Direct observation of electron transfer across a lipid bilayer: pulsed laser photolysis of an asymmetric vesicle system containing chlorophyll, methyl viologen, and EDTA, *Photochem. Photobiol.,* 35, 809, 1982.

81. **Ford, W. E. and Tollin, G.,** Chlorophyll photosensitized electron transfer in phospholipid bilayer vesicle systems: effects of cholesterol on radical yields and kinetic parameters, *Photochem. Photobiol.*, 40, 249, 1984.
82. **Hiromitsu, I. and Kevan, L.,** Correlation between photoexcited triplet state yield and photoionization yield of chlorophyll a in frozen phosphatidylcholine vesicles studied by electron spin resonance spectroscopy, *J. Phys. Chem.*, 93, 3218, 1989.
83. **Hotchandani, S., Leblanc, R. M., Clarke, R. H., and Fragata, M.,** Zero field optical detection of magnetic resonance of triplet states of chlorophyll a in lipid bilayer vesicles, *Photochem. Photobiol.*, 36, 235, 1982.
84. **Hiromitsu, I. and Kevan, L.,** Chlorophyll a triplet state ESR in frozen phosphatidylcholine vesicles, *J. Phys. Chem.*, 92, 2770, 1988.
85. **Clarke, R. H., Hanlon, E. B., and Boxer, S. G.,** Investigation of the lowest triplet state of the pyrochlorophyllide a-apomyoglobin complex by zero-field optically detected magnetic resonance spectroscopy, *Chem. Phys. Lett.*, 89, 41, 1982.
86. **Beck, J., von Schütz, J. U., and Wolf, H. C.,** Optically detected magnetic resonance of porphyrin complexes in the bacterium Rhodopseudomonas sphaeroides, *Z. Naturforsch. Teil C*, 38, 220, 1983.
87. **Hala, J., Searle, G. F. W., Schaafsma, T. J., van Hoek, A., Pančoška, P., Blaha, K., and Vaček, K.,** Picosecond laser spectroscopy and optically detected magnetic resonance on a model photosynthetic system, *Photochem. Photobiol.*, 44, 527, 1986.
88. **Wraight, C. A. and Boxer, S. G.,** Solution properties of synthetic chlorophyllide- and bacteriochlorophyllide-apomyoglobin complexes, *Biochemistry*, 20, 7546, 1981.
89. **Jones, O. T. G.,** Biosynthesis of porphyrins, hemes, and chlorophylls, in *The Photosynthetic Bacteria*, Clayton, R. K. and Sistrom, W. R., Eds., Plenum Press, New York, 1978, 751.
90. **Clarke, R. H. and Hanlon, E. B.,** ODMR and resonance Raman spectroscopy of chlorophyll *b* on graphite, *J. Chem. Phys.*, 82, 5275, 1985.
91. **Clarke, R. H., Graham, D. J., and Hanlon, E. B.,** Triplet state ODMR of molecules adsorbed to the surfaces of bulk metals, in *Photochemistry and Photobiology*, Vol. 2, Zewail, A. H., Ed., Harwood, London, 1983, 1011.
92. **Pac, C. and Ishitani, O.,** Yearly review: electron-transfer organic and bioorganic photochemistry, *Photochem. Photobiol.*, 48, 767, 1988.
93. **Closs, G. L., Forbes, M. D. E., and Norris, J. R.,** Spin-polarized electron paramagnetic resonance spectra of radical pairs in micelles. Observation of electron spin-spin interactions, *J. Phys. Chem.*, 91, 3592, 1987.
94. **Buckley, C. D., Hunter, D. A., Hore, P. J., and McLaughlan, K. A.,** Electron spin resonance of spin-correlated radical pairs, *Chem. Phys. Lett.*, 135, 307, 1987.
95. **Brown, R. G., Harriman, A., and Harris, L.,** Quenching of triplet chlorophyll a by aromatic nitrogen compounds, *J. Chem. Soc. Faraday Trans. 2*, 74, 1193, 1978.
96. **Andreeva, N. E., Zakharova, G. V., Shubin, V. V., and Chibisov, A. K.,** The role of the triplet state in chlorophyll photooxidation, *Chem. Phys. Lett.*, 53, 317, 1978.
97. **van Willigen, H., Vuolle, M., and Dinse, K. P.,** Time-resolved electron spin resonance study of photooxidation of zinc tetraphenylporphyrine by benzoquinone, *J. Phys. Chem.*, 93, 2441, 1989.
98. **den Blanken, H. J., van der Zwet, G. P., and Hoff, A. J.,** ESR in zero field of the photoinduced triplet state in isolated reaction centers of *Rhodopseudomonas sphaeroides* R-26 detected by singlet ground-state absorbance, *Chem. Phys. Lett.*, 85, 335, 1985.
99. **Hoff, A. J. and Gorter de Vries, H.,** Electron spin resonance in zero field of the reaction center triplet of photosynthetic bacteria, *Biochim. Biophys. Acta*, 503, 94, 1978.
100. **Clarke, R. H., Connors, R. E., Norris, J. R., and Thurnauer, M. C.,** Optically detected zero field magnetic resonance studies of the photoexcited triplet state of the photosynthetic bacterium *Rhodospirillum rubrum*, *J. Am. Chem. Soc.*, 89, 7178, 1975.
101. **Hoff, A. J., den Blanken, H. J., Vasmel, H., and Meiburg, R. F.,** Linear dichroic triplet-minus-singlet absorbance difference spectra of reaction centers of the photosynthetic bacteria *Chromatium vinosum*, *Rhodopseudomonas sphaeroides* R-26 and *Rhodospirillum rubrum* S1, *Biochim. Biophys. Acta*, 806, 389, 1985.
102. **Nishi, N., Schmidt, J., Hoff, A. J., and van der Waals, J. H.,** Fluorescence detection of electron spin echoes in the triplet state of non-phosphorescent molecules and in a photosynthetic bacterium, *Chem. Phys. Lett.*, 56, 205, 1978.
103. **Lous, E. J. and Hoff, A. J.,** Absorbance detected electron spin echo spectroscopy of non-radiative triplet states in zero field. An application to the primary donor in *Rhodobacter sphaeroides* R-26, *Chem. Phys. Lett.*, 140, 620, 1987.
104. **den Blanken, H. J., Vasmel, H., Jongenelis, A. P. J. M., Hoff, A. J., and Amesz, J.,** The triplet state of the primary donor of the green photosynthetic bacterium *Chloroflexus aurantiacus*, *FEBS Lett.*, 161, 185, 1983.

105. **den Blanken, H. J., van der Zwet, G. P., and Hoff, A. J.,** Study of the long-wavelength fluorescence band at 920 nm of isolated reaction centers of the photosynthetic bacterium *Rhodopseudomonas* R-26 with fluorescence detected magnetic resonance in zero magnetic field, *Biochim. Biophys. Acta*, 681, 375, 1982.
106. **Frank, H. A., Bolt, J., Friesner, R., and Sauer, K.,** Magnetophotoselection of the triplet state of reaction centers from *Rhodopseudomonas sphaeroides* R-26, *Biochim. Biophys. Acta*, 547, 502, 1979.
107. **Clarke, R. H., Connors, R. E., and Frank, H. A.,** Investigation of the structure of the reaction center in photosynthetic bacteria by optical detection of triplet state magnetic resonance, *Biochem. Biophys. Res. Commun.*, 71, 671, 1976.
108. **Gast, P. and Hoff, A. J.,** Determination of the decay rates of the triplet state of *Rhodopseudomonas sphaeroides* by fast laser-flash ESR spectroscopy, *FEBS Lett.*, 55, 183, 1978.
109. **Hoff, A. J.,** Kinetics of populating and depopulating of the components of the photoinduced triplet state of the photosynthetic bacteria *Rhodospirillum rubrum, Rhodopseudomonas sphaeroides* (wild-type), and its mutant R-26 as measured by ESR in zero field, *Biochim. Biophys. Acta*, 440, 765, 1976.
110. **Clarke, R. H. and Connors, R. E.,** Optically detected zero-field triplet state magnetic resonance in photosynthetic bacteria, *Chem. Phys. Lett.*, 42, 69, 1976.
111. **Beese, D., Steiner, R., Scheer, H., Angerhofer, A., Robert, B., and Lutz, M.,** Chemically modified photosynthetic bacterial reaction centers: circular dichroism, Raman resonance, low temperature absorption, fluorescence and ODMR spectra and polypeptide composition of borohydride treated reaction centers of *Rhodobacter sphaeroides* R-26, *Photochem. Photobiol.*, 47, 293, 1988.
112. **den Blanken, H. J., Jongenelis, A. P. J. M., and Hoff, A. J.,** The triplet state of the primary donor of the photosynthetic bacterium *Rhodopseudomonas viridis, Biochim. Biophys. Acta*, 725, 472, 1983.
113. **Dijkman, J. A., den Blanken, H. J., and Hoff, A. J.,** Towards a new taxonomy of photosynthetic bacteria: ADMR-monitored triplet difference spectroscopy of photosynthetic reaction center pigment protein complexes, *Isr. J. Chem.*, 28, 141, 1988.
114. **Beck, J., von Schütz, J. U., and Wolf, H. C.,** Fluorescence-ODMR of chlorophyll in photosynthetic bacteria. Reaction center of *Rhodopseudomonas sphaeroides* R-26, *Chem. Phys. Lett.*, 94, 141, 1983.
115. **Vasmel, H., den Blanken, H. J., Dijkman, J. T., Hoff, A. J., and Amesz, J.,** Triplet-minus-singlet absorbance difference spectra of reaction centers and antenna pigments of the green photosynthetic bacterium *Prosthecochloris aestuarii, Biochim. Biophys. Acta*, 767, 200, 1984.
116. **Angerhofer, A., von Schütz, J. U., and Wolf, H. C.,** Fluorescence-ODMR of reaction centers of *Rps. viridis, Z. Naturforsch. Teil C*, 39, 1085, 1984.
117. **Hoff, A. J. and Gorter de Vries, H.,** Energy transfer at 1.5 K in some photosynthetic bacteria monitored by microwave-induced fluorescence (MIF) spectra, *Isr. J. Chem.*, 21, 277, 1981.
118. **Prince, R. C., Dutton, P. L., Clayton, B. J., and Clayton, R. K.,** EPR properties of the reaction center of *Rhodopseudomonas gelatinosa* in situ and in a detergent-solubilized form, *Biochim. Biophys. Acta*, 502, 354, 1978.
119. **Prince, R. C.,** The reaction center and associated cytochromes of *Thiocapsa pfennigii:* their thermodynamic and spectroscopic properties, and their possible location within the photosynthetic membrane, *Biochim. Biophys. Acta*, 501, 195, 1978.
120. **Prince, R. C., Leigh, J. S., and Dutton, P. L.,** Thermodynamic properties of the reaction center of *Rhodopseudomonas viridis*. In vivo measurement of the reaction center bacteriochlorophyll-primary acceptor intermediary electron carrier, *Biochim. Biophys. Acta*, 440, 622, 1976.
121. **Beck, J., von Schütz, J. U., and Wolf, H. C.,** Fluorescence-ODMR of chlorophylls in photosynthetic bacteria. LH-I antenna complexes of *Rhodopseudomonas capsulata* Ala^+pho^-, *Chem. Phys. Lett.*, 94, 147, 1983.
122. **Angerhofer, A., von Schütz, J. U., and Wolf, H. C.,** Optical excited triplet states in antenna complexes of the photosynthetic bacterium *Rhodopseudomonas capsulata* Ala^+ detected by magnetic resonance in zero-field, in *Progress in Photosynthetic Research, Proc. 7th Int. Conf. Photosynthesis*, Vol. 1, Biggins, J., Ed., Martinus Nijhoff, Dordrecht, 1987, 4.427.
123. **Angerhofer, A., von Schütz, J. U., and Wolf, H. C.,** Fluorescence-ODMR of light harvesting pigments of photosynthetic bacteria, *Z. Naturforsch. Teil C*, 40, 379, 1985.
124. **Angerhofer, A.,** Optische und ODMR-Untersuchungen an Antennen und Reaktionszentren photosynthetisierender Bakterien, Ph.D. thesis, Universität Stuttgart, Stuttgart, Germany, 1987.
125. **Uphaus, R. A., Norris, J. R., and Katz, J. J.,** Triplet states in photosynthesis, *Biochem. Biophys. Res. Commun.*, 61, 1057, 1974.
126. **Hoff, A. J. and van der Waals, J. H.,** Zero field resonance and spin alignment of the triplet state of chloroplasts at 2° K, *Biochim. Biophys. Acta*, 423, 615, 1976.
127. **Hoff, A. J., Govindjee, and Romijn, J. C.,** Electron spin resonance in zero magnetic field of triplet states of chloroplast and subchloroplast particles, *FEBS Lett.*, 73, 191, 1977.
128. **Frank, H. A., McLean, M. B., and Sauer, K.,** Triplet states in photosystem I of spinach chloroplasts and subchloroplast particles, *Proc. Natl. Acad. Sci. U.S.A.*, 76, 5124, 1979.
129. **Clarke, R. H., Leenstra, W. R., and Hagar, W. G.,** Observation of a triplet state in chlorophyll protein 668 via optically detected magnetic resonance, *FEBS Lett.*, 99, 207, 1979.

130. **Leigh, J. S. and Dutton, P. L.,** Reaction center chlorophyll triplet state: redox potential dependence and kinetics, *Biochim. Biophys. Acta*, 357, 67, 1974.
131. **Nissani, E., Scherz, A., and Levanon, H.,** The photoexcited triplet state of tetraphenyl chlorin, magnesium tetraphenyl porphyrin and whole cells of *Chlamydomonas reinhardii*. A light modulation-EPR study, *Photochem. Photobiol.*, 25, 93, 1977.
132. **Rutherford, A. W., Paterson, D. R., and Mullet, J. E.,** A light-induced spin-polarized triplet detected by EPR in photosystem II reaction centers, *Biochim. Biophys. Acta*, 635, 205, 1981.
133. **Rutherford, A. W. and Mullet, J.,** Reaction center triplet states in photosystem I and photosystem II, *Biochim. Biophys. Acta*, 635, 225, 1981.
134. **Setif, P., Quagebeur, J.-P., and Mathis, P.,** Primary process in photosystem I. Identification and decay kinetics of the P-700 triplet state, *Biochim. Biophys. Acta*, 681, 345, 1982.
135. **Schaafsma, T. J., Searle, G. F. W., and Koehorst, R. B. M.,** Fluorescence detected triplet states in chlorophyll proteins, *J. Mol. Struct.*, 79, 461, 1982.
136. **den Blanken, H. J. and Hoff, A. J.,** High resolution absorbance difference spectra of the triplet state of the primary donor P-700 in photosystem I subchloroplast particles measured with absorbance detected magnetic resonance at 1.2 K. Evidence that P-700 is a dimeric chlorophyll complex, *Biochim. Biophys. Acta*, 724, 52, 1983.
137. **Gast, P., Swarthoff, T., Ebskamp, F. C. R., and Hoff, A. J.,** Evidence for a new early acceptor in photosystem I of plants. An ESR investigation of reaction center triplet yield and of the reduced intermediary acceptors, *Biochim. Biophys. Acta*, 722, 163, 1983.
138. **McLean, M. B. and Sauer, K.,** The dependence of reaction center and antenna triplets on the redox state of photosystem I, *Biochim. Biophys. Acta*, 679, 384, 1982.
139. **den Blanken, H. J., Hoff, A. J., Jongenelis, A. P. J. M., and Diner, B. A.,** High-resolution triplet-minus-singlet absorbance difference spectrum of photosystem II particles, *FEBS Lett.*, 157, 21, 1983.
140. **Nechushtai, R., Nelson, N., Gonen, O., and Levanon, H.,** Photosystem I reaction center from *Masticogladus laminosus*. Correlation between reduction state of the iron-sulphur center and the triplet formation mechanism, *Biochim. Biophys. Acta*, 897, 35, 1985.
141. **Clarke, R. H., Jagannathan, S. P., and Leenstra, W. R.,** Optical-microwave double resonance spectroscopy of in vivo chlorophyll, in *Lasers in Photomedicine and Photobiology*, Pratesi, R. and Sacchi, C. A., Eds., Springer-Verlag, Berlin, 1980, 171.
142. **Searle, G. F. W., van Brakel, G. H., Vermaas, W. F. J., van Hoek, A., and Schaafsma, T. J.,** Chlorophyll triplets and energy transfer in isolated PSI chlorophyll proteins from blue-green algae, in *Photosynthesis I. Photophysical Processes—Membrane Energization*, Akoyunoglou, G., Ed., Balaban, Philadelphia, 1981, 129.
143. **van der Bent, S. J., Schaafsma, T. J., and Goedheer, J. C.,** Detection of triplet states in algae by zero-field resonance, *Biochem. Biophys. Res. Commun.*, 71, 1147, 1976.
144. **Deisenhofer, J., Epp, O., Miki, K., Huber, R., and Michel, H.,** X-ray structure analysis of a membrane protein complex. Electron density map at 3 Å resolution and a model of the chromophores of the photosynthetic reaction center from *Rhodopseudomonas viridis*, *J. Mol. Biol.*, 180, 385, 1984.
145. **Kooyman, R. P. H.,** Complexes and Aggregates of Chlorophylls, Ph.D. thesis, Agricultural University of Wageningen, Wageningen, The Netherlands, 1980.
146. **Norris, J. R., Budil, D. E., Gast, P., Chang, C.-H., El-Kabbani, O., and Schiffer, M.,** Correlation of paramagnetic states and molecular structure in bacterial photosynthetic reaction centers: the symmetry of the primary donor in *Rhodopseudomonas viridis* and *Rhodobacter sphaeroides* R-26, *Proc. Natl. Acad. Sci. U.S.A.*, 86, 4335, 1989.
147. **Frank, H. A., Machniki, J., and Felber, M.,** Carotenoid triplet states in photosynthetic bacteria, *Photochem. Photobiol.*, 35, 713, 1982.
148. **van Dorp, W. G., Schoemaker, W. H., Soma, M., and van der Waals, J. H.,** The lowest triplet state of free base porphin. Determination of its kinetics of populating and depopulating from microwave-induced transients in the fluorescence intensity, *Mol. Phys.*, 30, 1701, 1975.
149. **Clarke, R. H. and Hofeldt, R. H.,** Optically detected zero field resonance studies of the photoexcited triplet state of chlorophyll a and b, *J. Chem. Phys.*, 61, 4582, 1974.
150. **Chika, P. A. and Clarke, R. H.,** Triplet state intersystem crossing rates from optically detected magnetic resonance spectroscopy, *J. Magn. Res.*, 29, 535, 1978.
151. **Hoff, A. J. and Cornelissen, B.,** Microwave power dependence of triplet state kinetics as measured with fluorescence detected magnetic resonance in zero field. An application to the reaction center bacteriochlorophyll triplet in bacterial photosynthesis, *Mol. Phys.*, 45, 413, 1982.
152. **Speer, R.,** Zeitaufgelöste ADMR an Reaktionszentren photosynthetisierender Bakterien, Diploma thesis, Universität Stuttgart, Stuttgart, Germany, 1988.
153. **Beck, J.,** Optisch nachgewiesene magnetische Resonanz an Pigment-Protein Komplexen photosynthetisierender Bakterien, Ph.D. thesis, Universität Stuttgart, Germany, 1983.

154. **Greis, J.,** Temperaturabhängige ADMR (absorptions-detektierte magnetische Resonanz) im Nullfeld am Reaktionszentrum in photosynthetisierenden Bakterien, Diploma thesis, Universität Stuttgart, Stuttgart, Germany, 1988.
155. **Hoff, A. J. and Proskuryakov, I. I.,** Triplet EPR spectra of the primary electron donor of bacterial photosynthesis Between 15 and 296 K, *Chem. Phys. Lett.*, 115, 303, 1985.
156. **Proskuryakov, I. I. and Manikowski, Kh.,** Temperature dependence of the bacteriochlorophyll triplet state ESR spectrum in the *Rhodobacter sphaeroides* R-26 reaction centers, *Dokl. Akad. Nauk S.S.S.R.*, 297, 1250, 1987.
157. **Frank, H. A., Machniki, J., and Friesner, R.,** Energy transfer between the primary donor bacteriochlorophylls and carotenoid in *Rhodopseudomonas sphaeroides, Photochem. Photobiol.*, 38, 451, 1983.
158. **Hoff, A. J., Lous, E. J., Moehl, K. W., and Dijkman, J. A.,** Magneto-optical absorbance difference spectroscopy. A new tool for the study of radical recombination reactions. An application to bacterial photosynthesis, *Chem. Phys. Lett.*, 114, 39, 1985.
159. **Lous, E. J. and Hoff, A. J.,** Triplet-minus-singlet absorbance difference spectra of the reaction center of *Rhodopseudomonas sphaeroides* R-26 in the temperature range 24—290 K measured by magneto-optical difference spectroscopy (MODS), *Photosynth. Res.*, 9, 89, 1986.
160. **Lous, E. J. and Hoff, A. J.,** Isotropic and linear dichroic triplet-minus-singlet absorbance difference spectra of two carotenoid containing bacterial reaction centers in the temperature range 10—288 K. An analysis of bacteriochlorophyll-carotenoid triplet transfer, *Biochim. Biophys. Acta*, 974, 88, 1989.
161. **Ullrich, J., Angerhofer, A., von Schütz, J. U., and Wolf, H. C.,** Zero-field absorption ODMR of reaction centers of *Rhodobacter sphaeroides* at temperatures between 4.2 and 75 K, *Chem. Phys. Lett.*, 140, 416, 1987.
162. **Ullrich, J.,** Temperaturabhängige ADMR Untersuchungen an Triplettzuständen in den Reaktionszentren photosynthetisierender Bakterien, Ph.D. thesis, Universität Stuttgart, Stuttgart, Germany, 1988.
163. **Botter, B. J., Nonhof, C. J., Schmidt, J., and van der Waals, J. H.,** The "mini-exciton" in the $C_{10}H_8$ naphthalene pair in a $C_{10}D_8$ host as studied by electron spin echo and ODMR techniques, *Chem. Phys. Lett.*, 43, 210, 1976.
164. **van Wijk, F. G. H.,** Triplet State Dynamics of Chlorophylls in Reaction Centers and Model Systems, Ph.D. thesis, Landgebouwuniversiteit Wageningen, Wageningen, The Netherlands, 1987.
165. **Gast, P. and Norris, J.,** EPR detected triplet formation in a single crystal of reaction center protein from the photosynthetic bacterium *Rhodopseudomonas sphaeroides* R-26, *FEBS Lett.*, 177, 277, 1984.
166. **Ponte-Goncalves, A. M. and Spendel, W. U.,** Comments on the triplet-state spin polarization in photosynthetic bacteria, *Chem. Phys. Lett.*, 54, 611, 1978.
167. **de Groot, A., Lous, E. J., and Hoff, A. J.,** Magnetic interactions between the triplet state of the primary donor and the prereduced ubiquinone acceptor in reaction centers of the photosynthetic bacterium *Rhodopseudomonas sphaeroides* 2.4.1, *Biochim. Biophys. Acta*, 808, 13, 1985.
168. **van Wijk, F. G. H., Gast, P., and Schaafsma, T. J.,** Interaction of a third electron spin with the radical pair in the photosynthetic bacterium Rhodopseudomonas viridis monitored by the donor-triplet electron spin polarization, *Photobiochem. Photobiophys.*, 11, 95, 1986.
169. **van Wijk, F. G. H., Gast, P., and Schaafsma, T. J.,** The relation between the electron spin polarization of the donor triplet state of the photosynthetic reaction center from Rhodopseudomonas viridis and the redox state of the primary acceptor, *FEBS Lett.*, 206, 238, 1986.
170. **van Wijk, F. G. H., Beijer, C. B., Gast, P., and Schaafsma, T. J.,** The electron spin polarization of the donor triplet state in native and modified photosynthetic reaction centers from *Rhodobacter sphaeroides* R-26, *Photochem. Photobiol.*, 46, 1015, 1987.
171. **van Wijk, F. G. H. and Schaafsma, T. J.,** Electron spin polarization in the donor triplet state of bacterial photosynthetic reaction centers. I. Microsecond time-resolved EPR of Rhodopseudomonas reaction centers, *Biochim. Biophys. Acta*, 936, 236, 1988.
172. **Hore, P. J., Hunter, D. A., van Wijk, F. G. H., Schaafsma, T. J., and Hoff, A. J.,** Electron spin polarization of the donor triplet state of bacterial photosynthetic reaction centers. II. Anisotropic inversion of electron spin polarization in a three-spin model reaction centre, *Biochim. Biophys. Acta*, 936, 249, 1988.
173. **Livingston, R. and Fujimori, E.,** Some properties of the ground triplet state of chlorophyll and related compounds, *J. Am. Chem. Soc.*, 80, 5610, 1958.
174. **Linschitz, H. and Sarkanen, K.,** The absorption spectra and the decay kinetics of the metastable state of chlorophyll a and b, *J. Am. Chem. Soc.*, 80, 4826, 1958.
175. **Pekkarinen, L. and Linschitz, H.,** Studies on metastable states of porphyrins. II. Spectra and decay kinetics of tetraphenylporphine, zinc tetraphenylporphine and bacteriochlorophyll, *J. Am. Chem. Soc.*, 82, 2407, 1960.
176. **Mathis, P. and Setif, P.,** Near infra-red absorption spectra of the chlorophyll a cations and triplet state in vitro and in vivo, *Isr. J. Chem.*, 21, 316, 1981.
177. **Setif, P., Hervo, G., and Mathis, P.,** Flash-induced absorption changes in photosystem I. Radical pair or triplet state formation, *Biochim. Biophys. Acta*, 638, 257, 1981.

178. **Lous, E. J.,** Interactions Between Pigments in Photosynthetic Protein Complexes. An Optically-Detected Magnetic Resonance and Magnetic Field Effect Study, Ph.D. thesis, Rijksuniversiteit Leiden, Leiden, The Netherlands, 1988.
179. **Lous, E. J. and Hoff, A. J.,** Exciton interactions in reaction centers of the photosynthetic bacterium Rhodopseudomonas viridis probed by optical triplet-minus-singlet polarization spectroscopy at 1.2 K monitored through absorbance detected magnetic resonance, *Proc. Natl. Acad. Sci. U.S.A.*, 84, 6147, 1987.
180. **Knapp, E. W., Scherer, P. O. J., and Fischer, S. F.,** Model studies of low-temperature optical transitions of photosynthetic reaction centers. A-, LD-, CD-, ADMR-, and LD-ADMR-spectra for *Rhodopseudomonas viridis*, *Biochim. Biophys. Acta*, 852, 295, 1986.
181. **Scherer, P. O. J. and Fischer, S. F.,** Model studies of low-temperature optical transitions. II. *Rhodobacter sphaeroides* and *Chloroflexus aurantiacus*, *Biochim. Biophys. Acta*, 891, 157, 1987.
182. **Scherer, P. O. J. and Fischer, S. F.,** Application of exciton theory to optical spectra of sodium borohydride treated reaction centers from *Rhodobacter sphaeroides* R-26, *Chem. Phys. Lett.*, 137, 32, 1987.
183. **den Blanken, H. J. and Hoff, A. J.,** High-resolution optical absorption-difference spectra of the triplet state of the primary donor in isolated reaction centers of the photosynthetic bacteria *Rhodopseudomonas sphaeroides* R-26 and *Rhodopseudomonas viridis* measured with optically detected magnetic resonance at 1.2 K, *Biochim. Biophys. Acta*, 681, 365, 1982.
184. **den Blanken, H. J., Meiburg, R. F., and Hoff, A. J.,** Polarized triplet-minus-singlet absorbance difference spectra measured by absorbance-detected magnetic resonance. An application to photosynthetic reaction centers, *Chem. Phys. Lett.*, 105, 336, 1984.
185. **Smit, H. W. J., Amesz, J., and van der Hoeven, M. F. R.,** Electron transport and triplet formation in membranes of the photosynthetic bacterium *Heliobacterium chlorum*, *Biochim. Biophys. Acta*, 893, 232, 1987.
186. **Lendzian, F., van Willigen, H., Sastry, S., Möbius, K., Scheer, H., and Feick, R.,** Proton ENDOR study of the photoexcited triplet state P^T in *Rhodopseudomonas sphaeroides* R-26 photosynthetic reaction centers, *Chem. Phys. Lett.*, 118, 145, 1985.
187. **de Groot, A., Evelo, R., Hoff, A. J., de Beer, R., and Scheer, H.,** Electron spin echo envelope modulation (ESEEM) spectroscopy of the triplet state of the primary donor of ^{14}N and ^{15}N bacterial photosynthetic reaction centers and of ^{14}N and ^{15}N bacteriochlorophyll *a*, *Chem. Phys. Lett.*, 118, 48, 1985.
188. **Buma, W. J., Evelo, R. G., Groenen, E. J. J., Hoff, A. J., Nan, H. M., and Schmidt, J.,** The reaction centre triplet state of the photosynthetic bacterium *Rhodobacter sphaeroides* R-26: electron spin echo spectroscopy of a single crystal, *Chem. Phys. Lett.*, 142, 231, 1987.
189. **Woodbury, N. W., Becker, M., Middendorf, D., and Parson, W. W.,** Picosecond kinetics of the initial photosynthetic electron-transfer reactions in bacterial photosynthetic reaction centers, *Biochemistry*, 24, 7516, 1985.
190. **Michel-Beyerle, M. E., Plato, M., Deisenhofer, J., Michel, H., Bixon, M., and Jortner, J.,** Unidirectionality in charge separation in reaction centers of photosynthetic bacteria, *Biochim. Biophys. Acta*, 932, 52, 1988.
191. **Fischer, S. F., Nussbaum, I., and Scherer, P. O. J.,** Electron transfer in rigidly linked donor-acceptor systems, in *Antennas and Reaction Centers of Photosynthetic Bacteria: Structures, Interactions and Dynamics*, Vol. 42, Springer Series in Chemical Physics, Michel-Beyerle, M. E., Ed., Springer-Verlag, Berlin, 1985, 256.
192. **Jortner, J. and Michel-Beyerle, M. E.,** Concluding remarks: some aspects of energy transfer in reaction centers of photosynthetic bacteria, in *Antennas and Reaction Centers of Photosynthetic Bacteria: Structures, Interactions and Dynamics*, Vol. 42, Springer Series in Chemical Physics, Michel-Beyerle, M. E., Ed., Springer-Verlag, Berlin, 1985, 345.
193. **Haberkorn, R., Michel-Beyerle, M. E., and Marcus, R. A.,** On spin-exchange and electron-transfer rates in bacterial photosynthesis, *Proc. Natl. Acad. Sci. U.S.A.*, 70, 4185, 1979.
194. **Marcus, R. A.,** Superexchange versus an intermediate BChl mechanism in reaction centers of photosynthetic bacteria, *Chem. Phys. Lett.*, 133, 471, 1987.
195. **Marcus, R. A.,** An internal consistency test and its applications for the initial steps in bacterial photosynthesis, *Chem. Phys. Lett.*, 146, 13, 1988.
196. **Chekalin, S. V., Matveez, Ya. A., Shuropatov, A. Ya., Shuvalov, V. A., and Yartzev, A. P.,** Femtosecond spectroscopy of primary charge separation in modified reaction centers of *Rhodobacter sphaeroides* (R-26), *FEBS Lett.*, 216, 245, 1987.
197. **Fischer, S. F. and Scherer, P. O. J.,** On the early charge separation and recombination processes in bacterial reaction centers, *Chem. Phys. Lett.*, 115, 151, 1987.
198. **Scherer, P. O. J. and Fischer, S. F.,** On the initial charge separation in bacterial reaction centers: long-range electron transfer via an exciton-charge transfer (ECT) coupling mechanism, *Chem. Phys. Lett.*, 141, 179, 1987.
199. **Won, Y. and Friesner, R. A.,** On the viability of the superexchange mechanism in the primary charge separation step in bacterial photosynthesis, *Biochim. Biophys. Acta*, 935, 9, 1988.

200. **Moser, C. C., Alegria, G., Gunner, M. R., and Dutton, P. L.,** Interpretation of the electric field sensitivity of the primary charge separation in photosynthetic reaction centers, *Isr. J. Chem.*, 28, 133, 1988.
201. **Bixon, M., Michel-Beyerle, M. E., and Jortner, J.,** Formation dynamics, decay kinetics, and singlet-triplet splittings of the (bacteriochlorophyll dimer)$^+$(bacteriopheophytin)$^-$ radical pair in bacterial photosynthesis, *Isr. J. Chem.*, 28, 155, 1988.
202. **Michel-Beyerle, M. E., Bixon, M., and Jortner, J.,** Interrelationship between primary electron transfer dynamics and magnetic interactions in photosynthetic reaction centers, *Chem. Phys. Lett.*, 151, 188, 1988.
203. **Lersch, W. and Michel-Beyerle, M. E.,** Implications of spin dynamics for the charge recombination in iron-depleted and quinone-substituted reaction centers from *Rhodobacter sphaeroides* R-26, *Biochim. Biophys. Acta*, 891, 265, 1987.
204. **Bixon, M., Jortner, J., Michel-Beyerle, M. E., Ogrodnik, A., and Lersch, W.,** The role of the accessory bacteriochlorophyll in reaction centers of photosynthetic bacteria: intermediate acceptor in the primary electron transfer?, *Chem. Phys. Lett.*, 140, 626, 1987.
205. **Holzapfel, W., Finkel, U., Kaiser, W., Oesterhelt, D., Scheer, H., Stilz, H. U., and Zinth, W.,** Observation of a bacteriochlorophyll anion radical during the primary charge separation in a reaction center, *Chem. Phys. Lett.*, 160, 1, 1989.
206. **Ogrodnik, A., Rémy-Richter, N., Michel-Beyerle, M. E., and Feick, R.,** Observation of activationless recombination in reaction centers of *R. sphaeroides*. A new key to the primary electron transfer mechanism, *Chem. Phys. Lett.*, 135, 576, 1987.
207. **Kolaczkowski, S., Budil, D., and Norris, J.,** $^3(P^+I^-)$ life-time as measured by B_1 field dependent RYDMR triplet yield, in *Progress in Photosynthesis Research*, Vol. 1, Biggins, J., Ed., Martinus Nijhoff, Dordrecht, 1987, 213.
208. **Norris, J. R., Budil, D. E., Tiede, D. M., Tang, J., Kolaczkowski, S. V., Chang, C. H., and Schiffer, M.,** Relating structure to function in bacterial photosynthetic reaction centers, in *Progress in Photosynthesis Research*, Vol. 1, Biggins, J., Ed., Martinus Nijhoff, Dordrecht, 1987, 363.
209. **Moehl, K. W., Lous, E. J., and Hoff, A. J.,** Low-power, low-field RYDMR of the primary radical pair in photosynthesis, *Chem. Phys. Lett.*, 121, 22, 1985.
210. **Hunter, D. A., Hoff, A. J., and Hore, P. J.,** Theoretical calculations of RYDMR effects in photosynthetic bacteria, *Chem. Phys. Lett.*, 134, 6, 1987.
211. **Norris, J. R., Bowman, M. K., Budil, D., Tang, J., Wraight, C. A., and Closs, G. L.,** Magnetic characterization of the primary state of bacterial photosynthesis, *Proc. Natl. Acad. Sci. U.S.A.*, 79, 5532, 1982.
212. **Lersch, W. and Michel-Beyerle, M. E.,** Magnetic field effects in the recombination of radical ions in reaction centers of photosynthetic bacteria, *Chem. Phys.*, 78, 115, 1983.
213. **Ogrodnik, A., Lersch, W., Michel-Beyerle, M. E., Deisenhofer, J., and Michel, H.,** Spin dipolar interactions of radical pairs in photosynthetic reaction centers, in *Antennas and Reaction Centers of Photosynthetic Bacteria*, Vol. 42, Springer Series in Chemical Physics, Michel-Beyerle, M. E., Ed., Springer-Verlag, Berlin, 1985, 198.
214. **Greis, J., Angerhofer, A., von Schütz, J. U., Speer, R., Ullrich, J., and Wolf, H. C.,** Absorption detected magnetic resonance (ADMR) and holeburning measurements on reaction center triplet states of *Rhodobacter sphaeroides* R-26, in *Current Research in Photosynthesis, Proc. 8th Int. Congr. Photosynthesis*, Vol. 1, Baltscheffsky, M., Ed., Kluwer, Dordrecht, 1990, 1.145.
215. **Lersch, W., Lendzian, F., Lang, E., Feick, R., Möbius, K., and Michel-Beyerle, M. E.,** High-power RYDMR with a loop-gap resonator, *J. Magn. Res.*, 82, 143, 1989.
216. **Norris, J. R., Lin, C. P., and Budil, D. E.,** Magnetic resonance of ultrafast chemical reactions, *J. Chem. Soc. Faraday Trans. 1*, 83, 13, 1987.
217. **Hore, P. J., Hunter, D. A., McKie, C. D., and Hoff, A. J.,** Electron paramagnetic resonance of spin-correlated radical pairs in photosynthetic reactions, *Chem. Phys. Lett.*, 137, 495, 1987.
218. **Feezel, L. L., Gast, P., Smith, U. H., and Thurnauer, M. C.,** Electron spin polarization of P^+-870 Q^- observed in the reaction center protein of the photosynthetic bacterium *Rhodobacter sphaeroides* R-26. The effect of selective isotopic substitution at X- and Q-band microwave frequencies, *Biochim. Biophys. Acta*, 974, 149, 1989.
219. **McGlynn, S. P., Azumi, T., and Kinoshita, M.,** *Molecular Spectroscopy of the Triplet State*, Prentice-Hall, Englewood Cliffs, NJ, 1969.
220. **Tang, J. and Norris, J. R.,** Theoretical calculations of kinetics of the radical pair P^F state in bacterial photosynthesis, *Chem. Phys. Lett.*, 92, 136, 1982.
221. **Tang, J. and Norris, J. R.,** Theoretical calculations of microwave effects on the triplet yield in photosynthetic reaction centers, *Chem. Phys. Lett.*, 94, 77, 1983.
222. **Hore, P. J., Watson, E. T., Pedersen, J. B., and Hoff, A. J.,** Line-shape analysis of polarized electron paramagnetic resonance spectra of the primary reactants of bacterial photosynthesis, *Biochim. Biophys. Acta*, 849, 70, 1986.

223. **Broadhurst, R. W., Hoff, A. J., and Hore, P. J.,** Interpretation of the polarized electron paramagnetic resonance signal of plant photosystem I, *Biochim. Biophys. Acta*, 852, 106, 1986.
224. **Thurnauer, M. C. and Gast, P.,** Q-band (35 GHz) EPR results on the nature of A_1 and the electron spin polarization in photosystem I particles, *Photobiochem. Photobiophys.*, 9, 29, 1985.
225. **Petersen, J., Stehlik, D. M., Gast, P., and Thurnauer, M.,** Comparison of the spin polarized spectrum found in plant photosystem I and in iron-depleted bacterial reaction centers with time-resolved K-band EPR; evidence that the photosystem I acceptor A_1 is a quinone, *Photosynth. Res.*, 14, 15, 1987.
226. **Thurnauer, M. C., Feezel, L. L., Morris, A. L., Smith, U., and Norris, J. R.,** Factors affecting electron spin polarization in photosynthetic systems, in *Current Research in Photosynthesis, Proc. 8th Int. Congr. Photosynthesis*, Vol. 1, Baltscheffsky, M., Ed., Kluwer, Dordrecht, 1990, 1.181.
227. **Norris, J. R., Morris, A. L., Thurnauer, M. C., and Tang, J. H.,** A general model of electron spin polarization arising from the interaction of radical pairs, *J. Chem. Phys.*, 92, 4239, 1990.
228. **Bock, C. H., Stehlik, D., and Thurnauer, M. C.,** Experimental evidence for the anisotropic nature of the transient EPR spectrum from photosystem I observed in Cyanobacteria, *Isr. J. Chem.*, 28, 177, 1988.
229. **Bock, C. H., van der Est, A. J., Brettel, K., and Stehlik, D.,** Nanosecond electron transfer kinetics in photosystem I as obtained from transient EPR at room temperature, *FEBS Lett.*, 247, 91, 1989.
230. **Stehlik, D., Bock, C. H., and Petersen, J.,** Anisotropic electron spin polarization of correlated spin pairs in photosynthetic reaction centers, *J. Phys. Chem.*, 93, 1612, 1989.